Immunological characteristics of DCs cotransduced with gp100 and IL-12

We first analyzed the expression levels of MHC/costimulatory molecules by flow cytometry in DCs prepared with various combinations of AdRGD-gp100 and AdRGD-IL12 (Fig 3). In comparison with mock DCs, DCs transduced with AdRGD-gp100 alone exhibited upregulated expression of all tested surface marker molecules, which play critical roles in the sensitization/activation of T cells, as was seen in mature LPS/DCs. This result agreed with our previous report demonstrating that transduction using AdRGD, irrespective of the type of inserted transgene, could enhance the expression of MHC/costimulatory molecules on DCs.[7] In addition, enhanced expression of MHC class I, CD40 and CD86 was observed as a characteristic change in DCs cotransduced with AdRGD-gp100 and AdRGD-IL12 as well as DCs transduced with AdRGD-IL12 alone. As upregulation of these molecules was dependent on MOI of

combined AdRGD-IL12, the results suggested that the secreted IL-12 promoted maturation of DCs by an autocrine mechanism.

Next, we compared antigen presentation levels via MHC class I molecules by bioassay using T–T hybridoma, CD8-OVA 1.3 cells, between DCs transduced with various combinations of AdRGD-OVA, AdRGD-IL12, and AdRGD-Luc (Fig 4). In comparison with DCs transduced with AdRGD-OVA alone, DCs cotransduced with AdRGD-OVA and AdRGD-IL12 showed a slight decrease in IL-2 released from CD8-OVA 1.3 cells by vector dose-increase of combined AdRGD-IL12. The OVA-presentation levels in AdRGD-OVA-transduced DCs were not affected by the addition of exogenous recombinant murine IL-12 into culture media during the antigen-presentation assay (data not shown). In addition, an obvious decline in the OVA-presentation level was observed in DCs cotransduced with AdRGD-OVA and AdRGD-Luc, suggesting that competition may occur during a particular step of the MHC class I

Relative fluorescence intensity
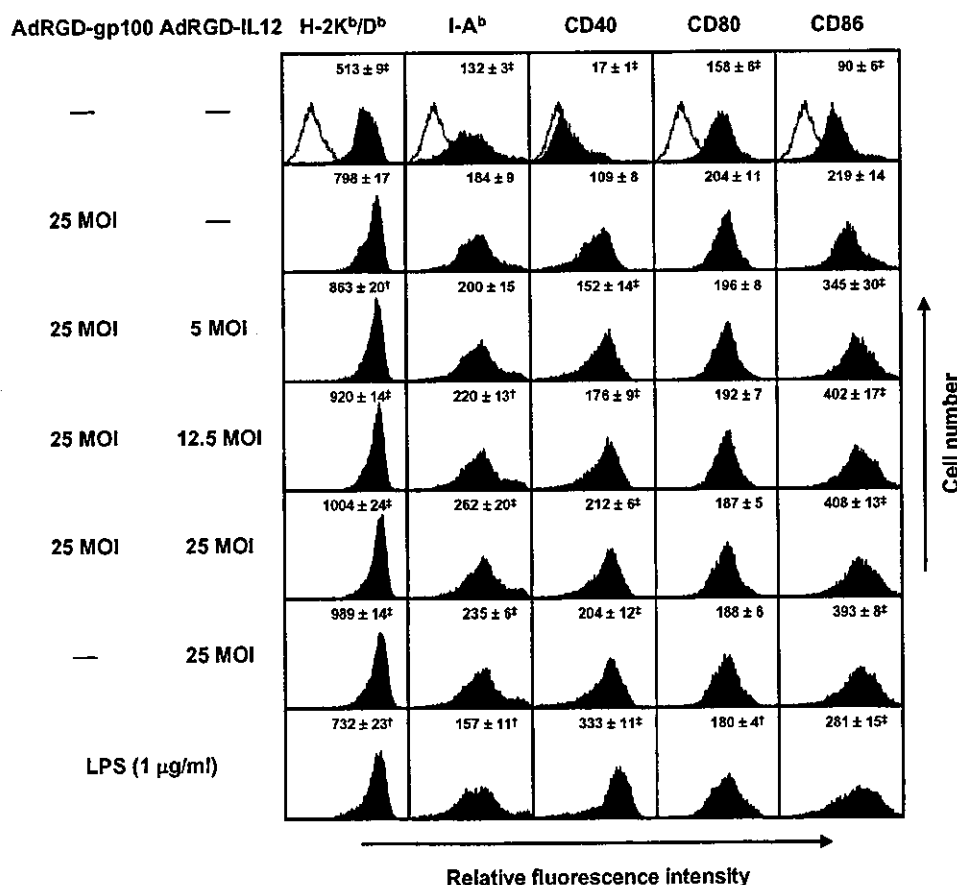
Figure 3 Flow cytometric analysis of surface markers in DCs cotransduced with gp100 and IL-12 gene by AdRGD. DCs were cotransduced with AdRGD-gp100 and AdRGD-IL12 at the indicated MOI for 2 hours. DCs treated with 1 μg/ml LPS for 24 hours were used as positive controls for phenotypical DC maturation. At 24 hours after transduction, cells were stained by indirect immunofluorescence using biotinylated mAbs of the indicated specificities (solid histogram). Dotted histograms represent cells stained by phycoerythrin-conjugated streptavidin alone. The data are representative of three independent experiments, and values indicated in the upper part of each panel represent MFI (mean±SD) of flow cytometric analysis. The statistical analysis was carried out by Student's t-test. $^\dagger P<.05$, $^\ddagger P<.01$ versus DCs transduced with AdRGD-gp100 alone at 25 MOI.
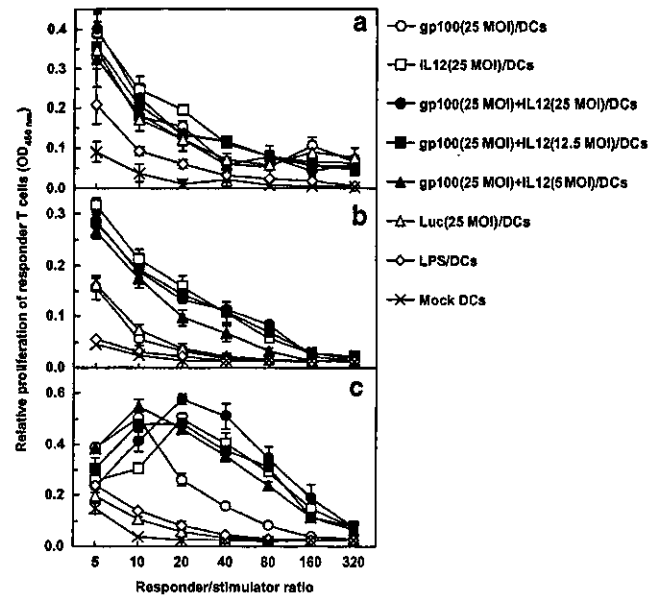
78
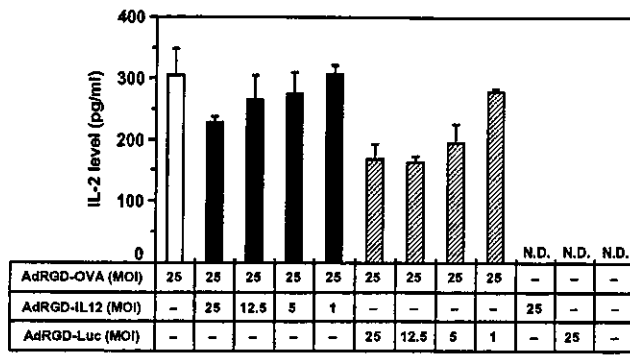
Figure 4 Antigen presentation on MHC class I molecules by DCs cotransduced with OVA and IL-12 gene by AdRGD. DCs were cotransduced with AdRGD-OVA and either AdRGD-IL12 or AdRGD-Luc at the indicated MOI for 2 hours. The levels of OVA peptide presentation via MHC class I molecules by transduced DCs were determined by bioassay using CD8-OVA 1.3 cells. The data represent the mean±SD of three independent cultures. ND: IL-2 secreted from CD8-OVA 1.3 cells was not detectable.

Figure 5 Allogeneic and syngeneic T-cell proliferation-stimulating ability of DCs cotransduced with gp100 and IL-12 gene by AdRGD. C57BL/6 DCs were transduced with the indicated combinations of various AdRGDs at the indicated MOI for 2 hours. Naive BALB/c T lymphocytes (a), naive C57BL/6 T lymphocytes (b), or gp100-primed C57BL/6 T lymphocytes (c), were cocultured with transduced, LPS-stimulated, or mock DCs at different responder/stimulator ratios for 3 days. Cell cultures were pulsed with BrdU during the last 18 hours, and then T-cell proliferation was assessed by BrdU-ELISA. Results are expressed as mean±SE of three independent cultures using T cells prepared from three individual mice.

antigen-presentation pathway in DCs simultaneously expressing distinct proteins due to the presence of multiple AdRGDs. The variation in effects of coexpressed endogenous antigens in DCs might be induced by proteins accumulating in the cytoplasm and secreted to extra-cellular fluid, such as luciferase and IL-12, respectively. Taken together, antigen-presenting levels via MHC class I molecules on DCs transduced with AdRGD encoding antigen were slightly decreased by increasing dose of combined AdRGD-IL12.

T-cell-stimulating ability of DCs cotransduced with gp100 and IL-12

We performed allogeneic and syngeneic MLR to compare T-cell proliferation-stimulating ability of DCs transduced with AdRGD-gp100 alone or a combination of AdRGD-gp100 and AdRGD-IL12. DCs transduced with AdRGD-gp100 alone at 25 MOI (gp100(25MOI)/DCs), AdRGD-IL12 alone at 25 MOI (IL12(25MOI)/DCs), AdRGD-Luc alone at 25 MOI (Luc(25MOI)/DCs), or various combinations of AdRGD-gp100 and AdRGD-IL12 (gp100 (25MOI) + IL12(25MOI)/DCs, gp100(25MOI) + IL12(12.5 MOI)/DCs, and gp100(25MOI) + IL12(5MOI)/DCs) could equally stimulate proliferation of allogeneic naive T cells used as responder cells (Fig 5a). In addition, T-cell proliferation levels in these groups were higher than those not only in mock DCs but also LPS/DCs. These data indicated that DCs transduced by using AdRGD could sufficiently provide proliferative stimuli to T cells through allogeneic interaction of MHC molecules/T-cell receptors and costimulatory signals, regardless of the quantity of IL-12 secreted from DCs. On the other hand, IL12(25-MOI)/DCs, gp100(25MOI) + IL12(25MOI)/DCs, gp100 (25MOI) + IL12(12.5MOI)/DCs, and gp100(25MOI) + IL12(5MOI)/DCs could more strongly stimulate syngeneic naive T-cell proliferation as compared with gp100(25MOI)/DCs or Luc(25MOI)/DCs (Fig 5b), suggesting that *in vitro* syngeneic naive T-cell proliferation by

DCs cotransduced with AdRGD-gp100 and AdRGD-IL12 was greatly influenced by secreted IL-12 rather than antigen-presentation via MHC molecules. Furthermore, in comparison with gp100(25MOI)/DCs, DCs transduced with AdRGD-IL12 alone or in combination with AdRGD-gp100 could induce considerable proliferation of syngeneic gp100-primed T cells, which were purified from C57BL/6 mice vaccinated beforehand with 10^6 gp100(25MOI)/DCs (Fig 5c). However, proliferation levels of syngeneic gp100-primed T cells stimulated by DCs transduced with AdRGD-IL12 alone or in combination with AdRGD-gp100 decreased at high responder/ stimulator ratios, and this suppressive effect became remarkable at high AdRGD-IL12 MOI during gene transduction. These observations suggested that excessive IL-12 secreted from transduced DCs might inhibit proliferation or induce cell death in activated T cells.

In addition, we assessed by ELISA the Th1/Th2 cytokine balance in media of syngeneic naive T cells cocultured with various transduced DCs for 5 days at a responder/stimulator ratio of 10 in the presence of 10 U/ml recombinant murine IL-2 (Table 1). IL12(25MOI)/DCs, gp100(25MOI) + IL12(25MOI)/DCs, gp100(25MOI) + IL12(12.5MOI)/DCs, and gp100(25MOI) + IL12(5MOI)/DCs could markedly enhance Th1-skewing IFN-γ secretion from syngeneic naive T cells as compared with mock

Table 1 Cytokine secretion from syngeneic naive T cells cocultured with various transduced DCs

| DC treatment				
AdRGD-gp100 (MOI)	AdRGD-IL12 (MOI)	IFN-γ (ng/ml)	IL-4 (pg/ml)	IL-10 (pg/ml)
—	—	0.25±0.05	<15	<30
25	—	1.00±0.19	<15	<30
—	25	17.17±0.48	<15	<30
25	25	25.78±1.84	<15	<30
25	12.5	18.61±1.47	<15	<30
25	5	20.23±2.96	<15	<30

Data are expressed as mean±SD of three independent cultures.

DCs, whereas only a slight increase in IFN-γ levels was observed during cocultivation with gp100(25MOI)/DCs. We confirmed that IFN-γ secretion was undetectable in control wells in which only transduced or mock DCs were cultured. On the other hand, secretion of the Th2 cytokines, IL-4 and IL-10, was not detectable in any syngeneic T cells stimulated by transduced or mock DCs. These results suggested that DCs cotransduced with gp100 and IL-12 could more efficiently differentiate sensitized T cells at the Th1-biasing state (the cellular immunity-dominant state), which is required for the induction of efficacious tumor immunity.

Vaccine efficacy of DCs cotransduced with gp100 and IL-12

In order to evaluate the potency of DCs cotransduced with gp100 and IL-12 as vaccine carriers, we investigated protective efficacy against murine B16BL6 melanoma challenge (Fig 6). C57BL/6 mice received a single intradermal injection of 2×10^5 DCs transduced with various combinations of AdRGD-gp100, AdRGD-IL12, and AdRGD-Luc, and then these mice were inoculated with 2×10^5 B16BL6 melanoma cells at 1 week post-immunization. Obvious growth suppression of the challenging B16BL6 tumor was achieved in mice vaccinated with gp100(25MOI)/DCs, as shown in our previous report,[9] whereas the mice immunized with IL12(25-MOI)/DCs or Luc(25MOI)/DCs showed little or no protective effect as compared with vehicle-injected mice. In addition, a more potent inhibitory effect on tumor growth could be observed in mice after vaccination with gp100(25MOI)+IL12(5MOI)/DCs than in mice vaccinated with gp100(25MOI)/DCs. However, vaccine efficacy of DCs cotransduced with gp100 and IL-12 tended to diminish with increasing AdRGD-IL12 MOI during gene transduction, and immunization with gp100(25MOI)+Luc(25MOI)/DCs led to inferior antitumor effects compared to those of the gp100(25MOI)/DCs group.

Furthermore, we investigated the cytolytic activities of NK cells and CTLs in mice intradermally immunized with DCs cotransduced with gp100 and IL-12 by Eu-release
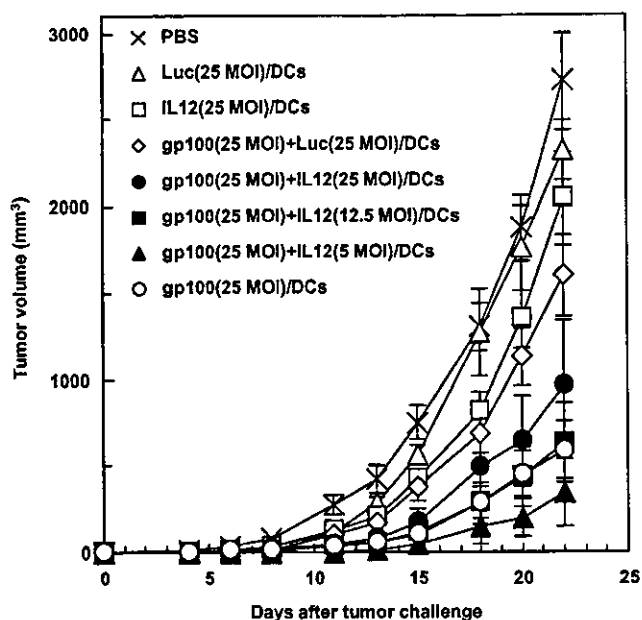
Figure 6 Vaccine efficacy of DCs cotransduced with gp100 and IL-12 gene by AdRGD against B16BL6 melanoma challenge. DCs were transduced with the indicated combinations of various AdRGDs at the indicated MOI for 2 hours. C57BL/6 mice were immunized by intradermal injection of transduced DCs into the left flank at 2×10^5 cells, and then 2×10^5 B16BL6 melanoma cells were inoculated into the right flank of the mice 1 week postvaccination. The size of tumors was assessed using microcalipers three times per week. Each point represents the mean±SE of 6–12 mice. Statistical analysis of tumor volume on day 22 after tumor challenge was carried out by Mann-Whitney U-test. P<.01 (■, ▲, O), P<.05 (●), not significant (×, □, ◇) versus Luc(25MOI)/DCs (△). P<.01 (×, △, □, ◇), not significant (●, ■, ▲) versus gp100(25MOI)/DCs (O).

assay. At 1 week after immunization of C57BL/6 mice with various DC vaccines, the splenocytes were used in a cytolytic assay against YAC-1 and EL4 cells, and were restimulated in vitro with inactivated B16BL6 cells, which were treated with recombinant murine IFN-γ to promote the expression of their MHC class I molecules, for CTL expansion. As shown in Figure 7a, the splenic cytolytic activity against YAC-1 cells markedly increased after immunization with gp100(25MOI)+IL12(25MOI)/DCs as well as IL12(25MOI)/DCs, whereas EL4 cells were not injured by splenocytes prepared from any groups. Effector cells from mice immunized with gp100(25MOI)+IL12(5MOI)/DCs exhibited equivalent NK activity to those from mice immunized with gp100(25MOI)/DCs. These data indicated that the non-specific NK activity involved in the anti-B16BL6 melanoma response was enhanced with the increase in IL-12 secretion from the administered DC vaccine. On the other hand, the cytolytic effects on B16BL6 cells by in vitro restimulated effector cells was promoted in mice immunized with gp100(25MOI)+IL12(5MOI)/DCs as compared with mice immunized with gp100(25MOI)/DCs (Fig 7b). This cytolytic activity was caused by B16BL6-specific CTLs because the effector cells prepared from

mice immunized with IL12(25MOI)/DCs or mock DCs did not injure the B16BL6 cells and no cytolytic effects against syngeneic irrelevant EL4 cells were detected in any
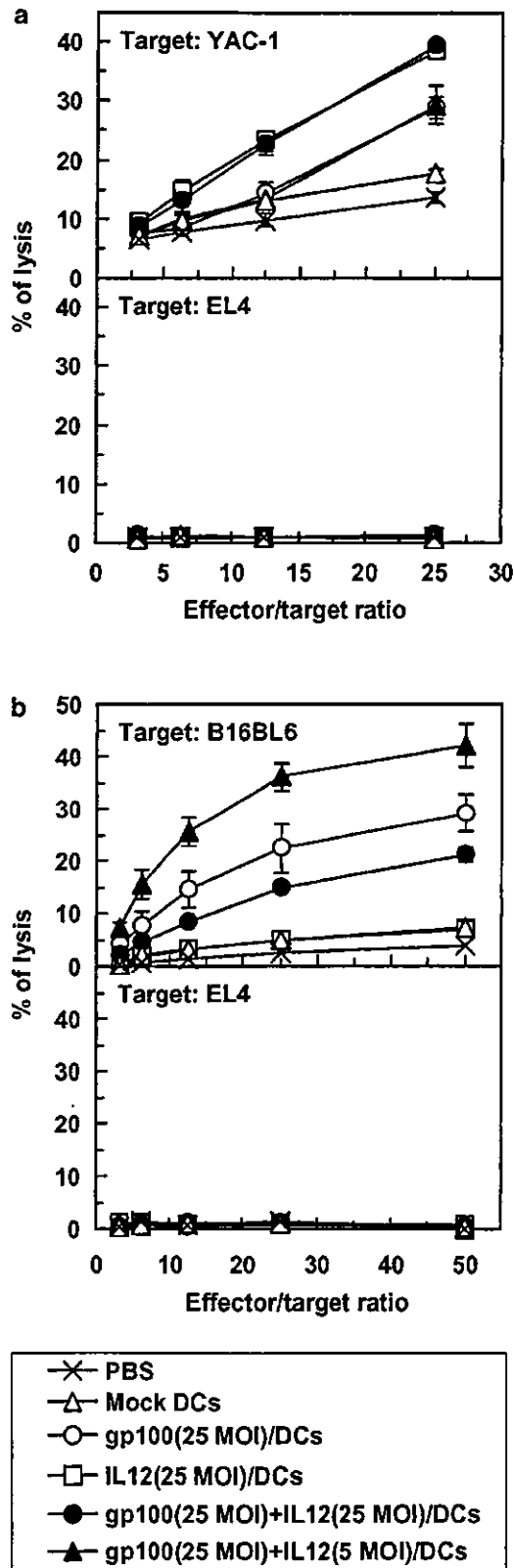
group. However, consistent with the protective effect against B16BL6 tumor challenge, mice vaccinated with gp100(25MOI) + IL12(25MOI)/DCs showed lower B16BL6-specific CTL activity than mice immunized with gp100(25MOI)/DCs.

Therefore, immunization with DCs genetically modified to express simultaneously gp100 and IL-12 exhibited duplicity for the host's immune response in our experimental model. That is, as compared with DCs transduced with AdRGD-gp100 alone, DCs cotransduced with AdRGD-IL12 at a relatively low ratio to AdRGD-gp100 were equal in inducibility of NK activity, but could more efficiently induce anti-B16BL6 tumor effects and antigen-specific CTL activity. In contrast, DCs combined with a high dose of AdRGD-IL12 during gene transduction could enhance NK activity, but attenuated B16BL6-protective efficacy and CTL activity.

Discussion

Since DCs are the most potent APCs and are uniquely capable of presenting novel antigens to naive T cells to initiate and modulate immune responses,[1,2] various DC-based vaccines for use in immune intervention strategies against cancer have been designed and studied in many research organizations. Antitumor CTLs play a central role in the tumor-specific immune response, and the efficient priming and subsequent activation of antitumor CTLs requires the processing and presentation of TAAs as peptide fragments in the context of appropriate MHC class I molecules by APCs.[31] In addition, a Th1-biased cytokine balance is desirable for sensitization of CTLs specific for TAA by APCs. IL-12 is the key factor that skews the immune balance toward a Th1 response and that can promote a switch from an established Th2 to a Th1 response.[32,33] In fact, potent antitumor effects of DCs genetically engineered with IL-12 have been demonstrated in several murine models by vaccination using TAA-derived peptide pulsed DCs or intratumoral injection using unpulsed DCs.[34–36] Therefore, we believe that, as compared with DCs delivered with TAA gene alone, DCs genetically manipulated to express simultaneously TAA and IL-12 might be a promising vaccine carrier

Figure 7 NK (a) and B16BL6-specific CTL (b) activity in mice immunized with DCs cotransduced with gp100 and IL-12 gene by AdRGD. DCs were transduced with the indicated combinations of AdRGD-gp100 and AdRGD-IL12 at the indicated MOI for 2 hours. Transduced or mock DCs were vaccinated once intradermally into C57BL/6 mice at 2×10^5 cells. At 1 week after immunization, nonadherent splenocytes were prepared from these mice, and directly used in cytolytic assays against YAC-1 and EL-4 cells (a). In addition, the isolated splenocytes were restimulated in vitro for 5 days with IFN-γ-stimulated and MMC-inactivated B16BL6 cells. A cytolytic assay using the restimulated splenocytes was performed against IFN-γ-stimulated B16BL6 and EL4 cells (b). Each point represents the mean ± SE of four independent cultures from four individual mice.

81

capable of generating more efficacious antitumor responses because of their ability to induce Th1-polarized responses.

A vector system, which can effectively deliver a foreign gene to DCs, is required to create a genetically modified DC vaccine having a potential to improve the efficacy of DC-based immunotherapy. We have demonstrated that AdRGD enabled highly efficient gene transduction into murine and human DCs because of the targeting of αv-integrin by the RGD sequence inserted at the HI-loop in their fiber knob.[6-9] When mouse bone marrow-derived DCs were cotransduced with AdRGD-gp100 and AdRGD-IL12, their expression of gp100 and IL-12 was comparable to that in DCs transduced with each AdRGD alone (Figs 1 and 2). IL-12 secreted from these DCs is biologically active because direct intratumoral injection of AdRGD-IL12, used in the present study and whose expression cassette was designed to be transcribed from IL-12p35 cDNA to the internal ribosome entry site sequence to IL-12p40 cDNA under the control of the cytomegalovirus promoter, could induce tumor regression based on promotion of tumor immunity in melanoma-bearing mice.[37] RT-PCR analysis (Fig 1) suggested that LPS-driven maturation or irrelevant AdRGD transduction could moderately enhance expression of the IL-12p40 subunit mRNA in DCs, but not IL-12p35 subunit mRNA. Several reports have demonstrated that the production of the two IL-12 subunits is regulated by different mechanisms, mainly at the level of mRNA expression, and that the level of bioactive IL-12p70 production in APCs in response to LPS and cytokines is determined by the level of IL-12p35 expression.[38,39] Therefore, DCs cannot attain sufficient IL-12p70 productivity, which is based on enhancement of endogenous gene expression of the two subunits, via a maturation signal from LPS or AdRGD transduction alone. Taken together, our results demonstrated that DCs cotransduced with AdRGD-gp100 and AdRGD-IL12 could simultaneously express gp100 and IL-12 at levels equal to DCs transduced with each vector alone, indicating that DCs can obtain several additional functions by using a combination of AdRGDs carrying different genes.

Full analysis and understanding of immunological characteristics of DC vaccine are imperative for the development of DC-based immunotherapy because the polarity of the immune response is greatly influenced by the activated state of DCs during T-cell sensitization. Flow cytometric analysis indicated that the expression of MHC class I/II, CD40, CD80, and CD86 molecules was enhanced only by AdRGD-transduction, and that DCs transduced with the IL-12 gene exhibited considerable upregulation of MHC class I, CD40, and CD86 molecules on their surface in response to autocrine effects of secreted IL-12 as compared with DCs transduced with AdRGD-gp100 alone (Fig 3). On the other hand, DCs cotransduced with OVA and IL-12 by AdRGDs exhibited lower OVA-presentation levels via MHC class I molecules than DCs transduced with AdRGD-OVA alone (Fig 4), although the cytoplasmic expression of endogenous antigen introduced into DCs was not affected by the

combination with other AdRGDs (Fig 2a). In addition, OVA-presentation levels in DCs transduced with AdRGD-OVA were markedly decreased by combination with AdRGD-Luc, which expresses luciferase as another endogenous antigen (Fig 4). These inconsistent results suggested that processing machineries in the MHC class I-presentation pathway may compete with multiple proteins transduced by the combination of AdRGDs, and that localization characteristics, such as cytoplasmic accumulation, extracellular secretion, and plasma membrane-specific localization, of other proteins should be considered during the preparation of DCs expressing TAA and other functional proteins by cotransduction with multiple AdRGDs in an attempt to maintain sufficient TAA-presenting capacity. With regard to T-cell-stimulating ability, DCs cotransduced with gp100 and IL-12 could more effectively enhance proliferation of syngeneic naive and gp100-primed T cells than DCs transduced with gp100 alone, although allogeneic T-cell proliferation did not differ between the two types of transduced DCs (Fig 5). Furthermore, we could detect considerable IFN-γ secretion from syngeneic naive T cells stimulated by DCs cotransduced with gp100 and IL-12 (Table 1), as expected. These data from *in vitro* immunological analysis suggested that DCs cotransduced with TAA and IL-12 using AdRGD can function as useful vaccine carriers possessing TAA-presentation ability, sufficient T-cell-stimulating ability, and Th1-driving ability *in vivo*.

We attempted to compare vaccine efficacy of DCs genetically modified with various combinations of AdRGD-gp100, AdRGD-IL12, and AdRGD-Luc using the murine B16BL6 melanoma model. Although mice vaccinated with gp100(25MOI)+IL12(5MOI)/DCs exhibited more effective suppression of B16BL6 tumor growth and efficient induction of B16BL6-specific CTLs than those vaccinated with gp100(25MOI)/DCs, vaccine efficacy of cotransduced DCs diminished with increasing combined AdRGD-IL12 MOI during gene transduction, contrary to our expectation (Figs 6 and 7). We speculated that this adverse effect might be caused by a decrease in antigen presentation in DCs by coexpression of TAA and IL-12 as shown in Figure 4, because the anti-B16BL6 effect of gp100(25MOI)+Luc(25MOI)/DCs was obviously inferior to that by gp100(25MOI)/DCs. An alternative explanation for the negative effect of AdRGD-IL12-cotransduction includes an immunosuppressive effect of excess IL-12 on the host's immune cells. Several studies have demonstrated that IL-12 inhibits cell-mediated immune responses, such as clonal expansion of CTLs, in a dose-dependent manner through IFN-γ-mediated nitric oxide production by macrophages in the murine models.[40-43] The *in vivo* bimodal effect of DCs cotransduced with gp100 and IL-12 in our model might involve immunosuppression based on nitric oxide, because DCs transduced with AdRGD-IL12 could drastically enhance IFN-γ secretion from syngeneic naive T cells in MLR (Table 1). In addition, Piccioli et al[44] reported that an *in vitro* interaction between activated NK cells and DCs at high NK/DC ratios resulted in inhibition of DC functions due to potent killing by NK cells,

whereas this interaction at low NK/DC ratios led to drastic increases in DC cytokine production. Therefore, a remarkable increase in NK activity in mice that were vaccinated with gp100(25MOI) + IL12(25MOI)/DCs, as shown in Figure 7, might suppress the induction of the B16BL6-specific immune response by the administered DC vaccine.

To date, vaccine efficacy of DCs cotransduced with TAA and IL-12 has not been fully clarified because both positive[45] and negative[46] effects of simultaneous expression of IL-12 in DC vaccine have been reported. Based on the results of the present study, we concluded that determination of the specific vector dose capable of optimizing both TAA-presentation levels and IL-12-secretion levels in DC vaccine is essential for improving antitumor efficacy based on active biasing of the immune response toward a cellular immunity dominated state.

Abbreviations

2-ME, 2-mercaptoethanol; AdRGD, RGD fiber-mutant adenovirus vector; APC, antigen-presenting cell; BrdU, 5-bromo-2'-deoxyuridine; CTL, cytotoxic T lymphocyte; DC, dendritic cell; Eu, europium; FBS, fetal bovine serum; GM-CSF, granulocyte/macrophage colony-stimulating factor; IFN, interferon; IL, interleukin; LPS, lipopolysaccharide; mAb, monoclonal antibody; MHC, major histocompatibility complex; MLR, mixed leukocyte reaction; MMC, mitomycin C; MOI, multiplicity of infection; NK, natural killer; OVA, ovalbumin; PBS, phosphate-buffered saline; RT-PCR, reverse transcription-polymerase chain reaction; TAA, tumor-associated antigen; Th, helper T cell.

Acknowledgments

References

1. Banchereau J, Steinman RM. Dendritic cells and the control of immunity. *Nature*. 1998;392:245–252.
2. Kapsenberg ML. Dendritic-cell control of pathogen-driven T-cell polarization. *Nat Rev Immunol*. 2003;3:984–993.
3. Nestle FO, Alijagic S, Gilliet M, et al. Vaccination of melanoma patients with peptide- or tumor lysate-pulsed dendritic cells. *Nat Med*. 1998;4:328–332.
4. Thurner B, Haendle I, Roder C, et al. Vaccination with mage-3A1 peptide-pulsed mature, monocyte-derived dendritic cells expands specific cytotoxic T cells and induces regression of some metastases in advanced stage IV melanoma. *J Exp Med*. 1999;190:1669–1678.
5. Yu JS, Wheeler CJ, Zeltzer PM, et al. Vaccination of malignant glioma patients with peptide-pulsed dendritic cells elicits systemic cytotoxicity and intracranial T-cell infiltration. *Cancer Res*. 2001;61:842–847.
6. Okada N, Tsukada Y, Nakagawa S, et al. Efficient gene delivery into dendritic cells by fiber-mutant adenovirus vectors. *Biochem Biophys Res Commun*. 2001;282:173–179.
7. Okada N, Masunaga Y, Okada Y, et al. Gene transduction efficiency and maturation status in mouse bone marrow-derived dendritic cells infected with conventional or RGD fiber-mutant adenovirus vectors. *Cancer Gene Ther*. 2003;10:421–431.
8. Okada N, Saito T, Masunaga Y, et al. Efficient antigen gene transduction using Arg-Gly-Asp fiber-mutant adenovirus vectors can potentiate antitumor vaccine efficacy and maturation of murine dendritic cells. *Cancer Res*. 2001;61:7913–7919.
9. Okada N, Masunaga Y, Okada Y, et al. Dendritic cells transduced with gp100 gene by RGD fiber-mutant adenovirus vectors are highly efficacious in generating anti-B16BL6 melanoma immunity in mice. *Gene Therapy*. 2003;10:1891–1902.
10. Hammerling GJ, Klar D, Pulm W, et al. The influence of major histocompatibility complex class I antigens on tumor growth and metastasis. *Biochim Biophys Acta*. 1987; 907:245–259.
11. Moller P, Hammerling GJ. The role of surface HLA-A,B,C molecules in tumour immunity. *Cancer Surv*. 1992;13: 101–127.
12. Khanna R. Tumour surveillance: missing peptides and MHC molecules. *Immunol Cell Biol*. 1998;76:20–26.
13. Nishimura T, Nakui M, Sato M, et al. The critical role of Th1-dominant immunity in tumor immunology. *Cancer Chemother Pharmacol*. 2000;46(Suppl):S52–S61.
14. Gubler U, Chua AO, Schoenhaut DS, et al. Coexpression of two distinct genes is required to generate secreted bioactive cytotoxic lymphocyte maturation factor. *Proc Natl Acad Sci USA*. 1991;88:4143–4147.
15. Wolf SF, Temple PA, Kobayashi M, et al. Cloning of cDNA for natural killer cell stimulatory factor, a hetero-dimeric cytokine with multiple biologic effects on T and natural killer cells. *J Immunol*. 1991;146:3074–3081.
16. Robertson MJ, Soiffer RJ, Wolf SF, et al. Response of human natural killer (NK) cells to NK cell stimulatory

factor (NKSF): cytolytic activity and proliferation of NK cells are differentially regulated by NKSF. *J Exp Med.* 1992;175:779–788.

17. Brunda MJ. Interleukin-12. *J Leukoc Biol.* 1994;55:280–288.
18. Chan SH, Perussia B, Gupta JW, et al. Induction of interferon gamma production by natural killer cell stimulatory factor: characterization of the responder cells and synergy with other inducers. *J Exp Med.* 1991;173:869–879.
19. Chan SH, Kobayashi M, Santoli D, et al. Mechanisms of IFN-γ induction by natural killer cell stimulatory factor (NKSF/IL-12). Role of transcription and mRNA stability in the synergistic interaction between NKSF and IL-2. *J Immunol.* 1992;148:92–98.
20. Hsieh CS, Macatonia SE, Tripp CS, et al. Development of TH1 CD4$^+$ T cells through IL-12 produced by Listeria-induced macrophages. *Science.* 1993;260:547–549.
21. Seder RA, Gazzinelli R, Sher A, et al. Interleukin 12 acts directly on CD4$^+$ T cells to enhance priming for interferon γ production and diminishes interleukin 4 inhibition of such priming. *Proc Natl Acad Sci USA.* 1993;90:10188–10192.
22. Nastala CL, Edington HD, McKinney TG, et al. Recombinant IL-12 administration induces tumor regression in association with IFN-γ production. *J Immunol.* 1994;153:1697–1706.
23. Voest EE, Kenyon BM, O'Reilly MS, et al. Inhibition of angiogenesis *in vivo* by interleukin 12. *J Natl Cancer Inst.* 1995;87:581–586.
24. Pfeifer JD, Wick MJ, Roberts RL, et al. Phagocytic processing of bacterial antigens for class I MHC presentation to T cells. *Nature.* 1993;361:359–362.
25. Mizuguchi H, Koizumi N, Hosono T, et al. A simplified system for constructing recombinant adenoviral vectors containing heterologous peptides in the HI loop of their fiber knob. *Gene Therapy.* 2001;8:730–735.
26. Okada Y, Okada N, Nakagawa S, et al. Fiber-mutant technique can augment gene transduction efficacy and antitumor effects against established murine melanoma by cytokine-gene therapy using adenovirus vectors. *Cancer Lett.* 2002;177:57–63.
27. Mizuguchi H, Kay MA. Efficient construction of a recombinant adenovirus vector by an improved *in vitro* ligation method. *Hum Gene Ther.* 1998;9:2577–2583.
28. Mizuguchi H, Kay MA. A simple method for constructing E1- and E1/E4-deleted recombinant adenoviral vectors. *Hum Gene Ther.* 1999;10:2013–2017.
29. Lutz MB, Kukutsch N, Ogilvie AL, et al. An advanced culture method for generating large quantities of highly pure dendritic cells from mouse bone marrow. *J Immunol Methods.* 1999;223:77–92.
30. Okada N, Tsujino M, Hagiwara Y, et al. Administration route-dependent vaccine efficiency of murine dendritic cells pulsed with antigens. *Br J Cancer.* 2001;84:1564–1570.
31. Lanzavecchia A. Identifying strategies for immune intervention. *Science.* 1993;260:937–944.
32. Scott P, Trinchieri G. IL-12 as an adjuvant for cell-mediated immunity. *Semin Immunol.* 1997;9:285–291.

33. Shurin MR, Esche C, Peron JM, et al. Antitumor activities of IL-12 and mechanisms of action. *Chem Immunol.* 1997;68:153–174.
34. Zitvogel L, Couderc B, Mayordomo JI, et al. IL-12-engineered dendritic cells serve as effective tumor vaccine adjuvants *in vivo*. *Ann NY Acad Sci.* 1996;795:284–293.
35. Nishioka Y, Hirao M, Robbins PD, et al. Induction of systemic and therapeutic antitumor immunity using intratumoral injection of dendritic cells genetically modified to express interleukin 12. *Cancer Res.* 1999;59:4035–4041.
36. Melero I, Duarte M, Ruiz J, et al. Intratumoral injection of bone-marrow derived dendritic cells engineered to produce interleukin-12 induces complete regression of established murine transplantable colon adenocarcinomas. *Gene Therapy.* 1999;6:1779–1784.
37. Okada Y, Okada N, Mizuguchi H, et al. Optimization of antitumor efficacy and safety of *in vivo* cytokine gene therapy using RGD fiber-mutant adenovirus vector for preexisting murine melanoma. *Biochim Biophys Acta.* 2004;1670:172–180.
38. Snijders A, Hilkens CM, van der Pouw Kraan TC, et al. Regulation of bioactive IL-12 production in lipopolysaccharide-stimulated human monocytes is determined by the expression of the p35 subunit. *J Immunol.* 1996;156:1207–1212.
39. Kalinski P, Vieira PL, Schuitemaker JH, et al. Prostaglandin E$_2$ is a selective inducer of interleukin-12 p40 (IL-12p40) production and an inhibitor of bioactive IL-12p70 heterodimer. *Blood.* 2001;97:3466–3469.
40. Koblish HK, Hunter CA, Wysocka M, et al. Immune suppression by recombinant interleukin (rIL)-12 involves interferon gamma induction of nitric oxide synthase 2 (iNOS) activity: inhibitors of NO generation reveal the extent of rIL-12 vaccine adjuvant effect. *J Exp Med.* 1998;188:1603–1610.
41. Medot-Pirenne M, Heilman MJ, Saxena M, et al. Augmentation of an antitumor CTL response *in vivo* by inhibition of suppressor macrophage nitric oxide. *J Immunol.* 1999;163:5877–5882.
42. Lasarte JJ, Corrales FJ, Casares N, et al. Different doses of adenoviral vector expressing IL-12 enhance or depress the immune response to a coadministered antigen: the role of nitric oxide. *J Immunol.* 1999;162:5270–5277.
43. Nishioka Y, Wen H, Mitani K, et al. Differential effects of IL-12 on the generation of alloreactive CTL mediated by murine and human dendritic cells: a critical role for nitric oxide. *J Leukoc Biol.* 2003;73:621–629.
44. Piccioli D, Sbrana S, Melandri E, et al. Contact-dependent stimulation and inhibition of dendritic cells by natural killer cells. *J Exp Med.* 2002;195:335–341.
45. Chen Y, Emtage P, Zhu Q, et al. Induction of ErbB-2/neu-specific protective and therapeutic antitumor immunity using genetically modified dendritic cells: enhanced efficacy by cotransduction of gene encoding IL-12. *Gene Therapy.* 2001;8:316–323.
46. Ribas A, Amarnani SN, Buga GM, et al. Immunosuppressive effects of interleukin-12 coexpression in melanoma antigen gene-modified dendritic cell vaccines. *Cancer Gene Ther.* 2002;9:875–883.

RESEARCH ARTICLE

Augmentation of the migratory ability of DC-based vaccine into regional lymph nodes by efficient CCR7 gene transduction

N Okada[1], N Mori[1], R Koretomo[1], Y Okada[2], T Nakayama[3], O Yoshie[3], H Mizuguchi[4], T Hayakawa[5], S Nakagawa[6], T Mayumi[6], T Fujita[1] and A Yamamoto[1]

[1]Department of Biopharmaceutics, Kyoto Pharmaceutical University, Misasagi, Yamashina-ku, Kyoto, Japan; [2]Research Institute for Microbial Diseases, Osaka University, Osaka, Japan; [3]Department of Microbiology, Kinki University School of Medicine, Osaka-Sayama, Osaka, Japan; [4]Division of Cellular and Gene Therapy Products, National Institute of Health Sciences, Setagaya-ku, Tokyo, Japan; [5]National Institute of Health Sciences, Setagaya-ku, Tokyo, Japan; and [6]Department of Biopharmaceutics, Graduate School of Pharmaceutical Sciences, Osaka University, Osaka, Japan

Although dendritic cell (DC)-based immunotherapy is considered a promising approach for cancer treatment, a large quantity of DC vaccine is required for effective sensitization/activation of immune cells because of the poor migratory ability of administered DCs into regional lymphoid tissue. In this study, we created a DC vaccine sufficiently transduced with CC chemokine receptor-7 gene (CCR7/DCs) by applying RGD fiber-mutant adenovirus vector (AdRGD), and investigated its immunological characteristics and therapeutic efficacy. CCR7/DCs acquired strong chemotactic activity for CC chemokine ligand-21 (CCL21) and exhibited an immunophenotype similar to mature DCs but not immature DCs with regard to major histocompatibility complex/costimulatory molecule-expression levels and allogenic T cell proliferation-stimulating ability, while maintaining inherent endocytotic activity. Importantly, CCR7/DCs injected intradermally into mice could accumulate in draining lymph nodes about 5.5-fold more efficiently than control AdRGD-applied DCs. Reflecting these properties of CCR7/DCs, DC vaccine genetically engineered to simultaneously express endogenous antigen and CCR7 could elicit more effective antigen-specific immune response in vivo using a lower dosage than DC vaccine transduced with antigen alone. Therefore, the application of CCR7/DCs having positive migratory ability to lymphoid tissues may contribute to reduction of efforts and costs associated with DC vaccine preparation by considerably reducing the DC vaccine dosage needed to achieve effective treatment by DC-based immunotherapy.
Gene Therapy (2005) 12, 129–139. doi:10.1038/sj.gt.3302358
Published online 14 October 2004

Keywords: dendritic cell-based vaccination; RGD fiber-mutant adenovirus vector; CCR7; migration; melanoma

Introduction

Immunotherapy using dendritic cells (DCs), which play a critical role in control of both acquired and innate immune responses in the living body, is studied energetically in many research organizations aiming to immunologically eradicate cancer. In addition, several cancer immunotherapy protocols using DC vaccine introduced with tumor-associated antigen (TAA) advanced to the clinical study phase.[1–4] However, since currently available DC-based immunotherapy has not demonstrated exceptional therapeutic effects in these clinical studies, the development of a novel approach capable of improving the efficacy of this promising strategy for cancer treatment is eagerly awaited.

DCs are widely distributed over peripheral tissues, where they catch invading antigens by full endocytotic activity, characteristic of an immature state. The pheno-type of DCs internalizing antigens changes to a mature state in response to these inflammatory stimuli. Subsequently, they process the antigens into the peptides presented on major histocompatibility complex (MHC) molecules, migrate into draining lymph nodes (LNs) via afferent lymphatic venules, and induce primary immune responses through antigen presentation to T cells.[5–7] On the basis of these serial immune mechanisms, the degree of administered DC vaccine accumulation in lymphoid tissues is a factor in enhancing or restricting therapeutic effects in DC-based immunotherapy.

In recent years, identification and functional analysis of chemokines/chemokine receptors, which regulate relevant leukocyte migration and invasion into tissues, have progressed remarkably, and the chemokine–chemokine receptor coupling in DC migration from peripheral tissue to lymphoid tissue has been elucidated. Gunn et al[8] found that DC migration to secondary lymphoid tissues was inhibited in CC chemokine ligand-21 (CCL21) expression-defective plt/plt mice. Likewise, Förster et al[9] reported that inhibition of DC migration to secondary lymphoid tissues occurred in CC chemokine receptor-7 (CCR7)-knockout mice. Based on these results, the association between CCL21, which is pro-

duced and secreted constitutively in lymphoid tissues and lymphatic vessels, and CCR7, a seven-transmembrane domain G-protein-coupled receptor whose expression is enhanced on the surface of maturing DCs, has been shown to play a central role in control of DC migration from the peripheral tissue to lymphoid tissues. Therefore, DCs, which are not only introduced with antigens but also exhibit enhanced CCR7 expression, may positively migrate to lymphoid tissue and efficiently activate the host's immune system after administration to a living body. Efficient CCR7-gene transduction to DCs is proposed as a preparatory method for this novel 'lymphoid tissue-directivity DC' vaccine.

Efficient gene transduction to DCs is difficult in any conventional vector system including adenovirus vector (Ad), which could transfect in a wide variety of cells and tissues.[10] In this regard, we succeeded in establishing highly efficient gene transduction to DCs by applying RGD fiber-mutant Ad (AdRGD),[11-14] and clarified that vaccination with DCs transduced with TAA gene using AdRGD induced considerable antitumor effect based on activation of TAA-specific cytotoxic T lymphocytes (CTLs) in mice.[12,14] Our results not only revealed that AdRGD is very useful in antigen gene delivery to DCs, but also opened up new potentiality for genetically enhancing the immunological functions of DCs by

making use of the predominance of AdRGD in gene transduction efficiency to DCs. Thus, in the present study, we first constructed an AdRGD-carrying CCR7 gene (AdRGD-CCR7), and investigated the immunological properties and vaccine efficacy of murine bone marrow-derived DCs modified with AdRGD-CCR7 in order to create a 'lymphoid tissue-directivity DC' vaccine.

Results

Gene transduction into DCs by AdRGD-CCR7

We examined the cytopathic effects of gene transduction using AdRGD-CCR7 to DCs by MTT assay. AdRGD-CCR7 did not injure DCs with a vector dose of 100 multiplicities of infection (MOI) or less, whereas viability of DCs was slightly reduced by using AdRGD-CCR7 at 200 MOI (data not shown). Thus, CCR7 gene expression was evaluated by semiquantitative reverse transcription-polymerase chain reaction (RT-PCR) analysis in DCs transduced with AdRGD-CCR7 at 100 MOI or less. The CCR7 mRNA level of lipopolysaccharide-stimulated DCs (LPS/DCs) or Luc/DCs transduced with AdRGD-Luc (luciferase-expressing control vector) at 50 MOI did not show a remarkable change in comparison with that of mock (immature) DCs at 24 h post-treatment (Figure 1a).
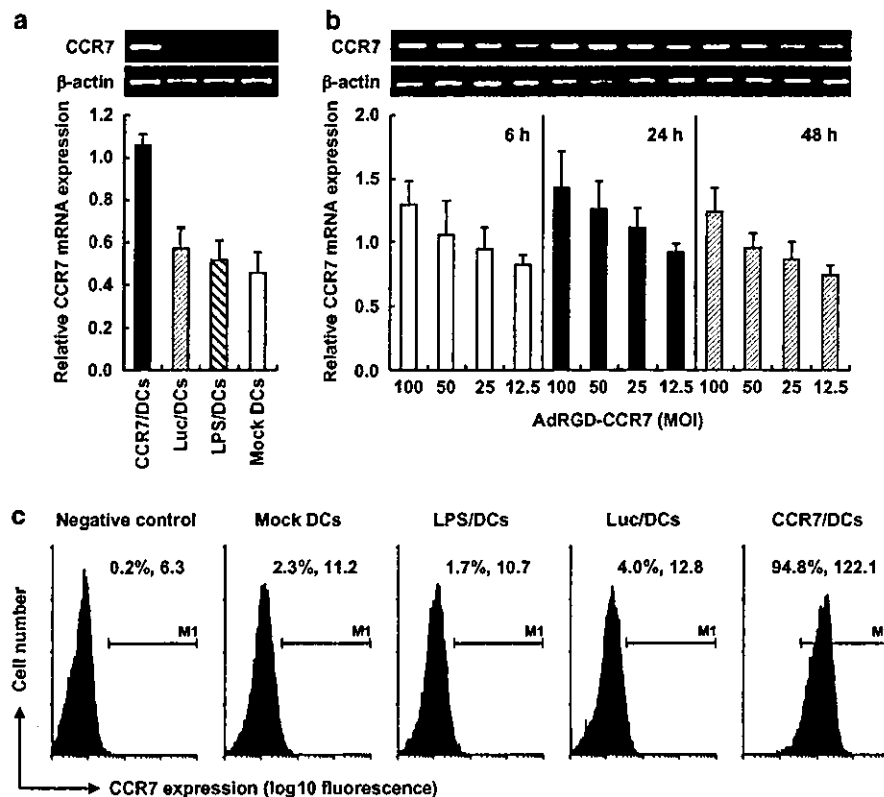
Figure 1 RT-PCR and flow cytometric analysis for mouse CCR7 expression levels. DCs were transduced with AdRGD-CCR7 or AdRGD-Luc at 50 MOI (a and c) or the indicated MOI (b). These transduced cells, LPS-stimulated DCs, and mock DCs were cultured for 24 h (a and c) or the indicated period (b) in GM-CSF-free medium. (a and b) Total RNA was isolated from these DCs, and then mouse CCR7 mRNA expression was assessed by RT-PCR analysis. Relative CCR7 mRNA expression was calculated as ratio of the densitometric units of PCR products derived from CCR7 transcripts to the densitometric units of PCR products derived from β-actin transcripts. Data are presented as mean ± s.d. of results from three independent experiments. (c) Flow cytometric analysis was performed by using anti-mouse CCR7 antibody. Negative control represents mock DCs stained by second antibody alone. The data are representative of two independent experiments, and the % value and the numerical value indicated in the upper part of each panel express % of M1-gated cells and mean fluorescence intensity (MFI), respectively.

On the other hand, CCR7/DCs prepared with AdRGD-CCR7 at 50 MOI were able to express CCR7 mRNA at a level more than double that of mock DCs. In addition, we analyzed the changes in CCR7 mRNA expression over time in CCR7/DCs transduced at various vector doses (Figure 1b). It was revealed that CCR7 mRNA expression in CCR7/DCs increased in a vector dose-dependent manner, and highest levels were observed at 24 h after gene transduction. Moreover, flow cytometric analysis using anti-mouse CCR7 polyclonal antibody showed that most of the CCR7/DCs, which were prepared with AdRGD-CCR7 at 50 MOI and then cultured for 24 h, expressed CCR7 protein on their surface, whereas few CCR7-positive cells were detected in mock DCs, LPS/DCs, and Luc/DCs (Figure 1c).

Next, we evaluated the chemotactic activity of CCR7/DCs for CCL21 by *in vitro* chemotaxis assay in order to confirm functional CCR7 expression on the cell surface. Under transductional conditions at an MOI of 50, the number of migrating CCR7/DCs cultured for 24 h markedly increased with increasing CCL21 concentration, whereas Luc/DCs, LPS/DCs, and mock DCs remained at low levels despite CCL21 stimulation (Figure 2a). Furthermore, as was observed for RT-PCR analysis in Figure 1b, the chemotactic activity of CCR7/DCs for CCL21 was enhanced with increasing AdRGD-CCR7 dose during transduction (Figure 2b). These results clearly demonstrated that functional CCR7, which could promote migration of DCs in response to a CCL21 concentration gradient, was expressed on the CCR7/DC surface, and that transduction of the chemokine receptor gene by AdRGD could modify chemokine responsiveness of DCs.

Immunological properties of CCR7/DCs

We analyzed the immunological characteristics of CCR7/DCs prepared with AdRGD-CCR7 at 50 MOI. At first, the expression levels of MHC/costimulatory molecules in CCR7/DCs cultured for 24 h were analyzed by flow cytometry (Figure 3a). In comparison with mock DCs, CCR7/DCs and Luc/DCs exhibited upregulated expression of all tested surface marker molecules, which play critical roles in the sensitization/activation of T cells, as is seen in mature LPS/DCs. In particular, the expression levels of CD40 and CD86 were dramatically enhanced by gene transduction using AdRGD. This result agreed with our previous report demonstrating that transduction using AdRGD, irrespective of the type of inserted transgene, could enhance the expression of MHC/costimulatory molecules on DCs.[13] Moreover, CCR7/DCs were able to stimulate proliferation of allogenic naive T cells in mixed leukocyte reaction (MLR) more effectively than mock DCs, and the stimulatory ability of CCR7/DCs, Luc/DCs, and LPS/DCs was equal at a responder/stimulator ratio of 5 (Figure 3b).

The level of fluorescein isothiocyanate (FITC)-dextran uptake in CCR7/DCs was estimated as an index of their endocytotic activity (Figure 3c). Excellent endocytosis for FITC-dextran was observed in mock DCs incubated at 37°C, whereas fluorescence intensity derived from internalized FITC-dextran was drastically decreased by 4°C incubation or LPS-driving maturation. On the other hand, FITC-dextran-uptake levels in CCR7/DCs and Luc/DCs, which were cultured for 24 h after gene transduction, were comparable to those in mock DCs.
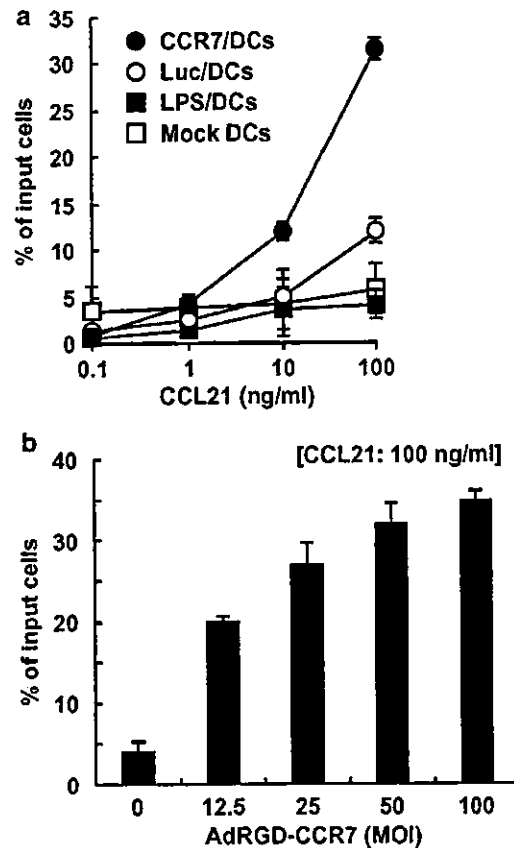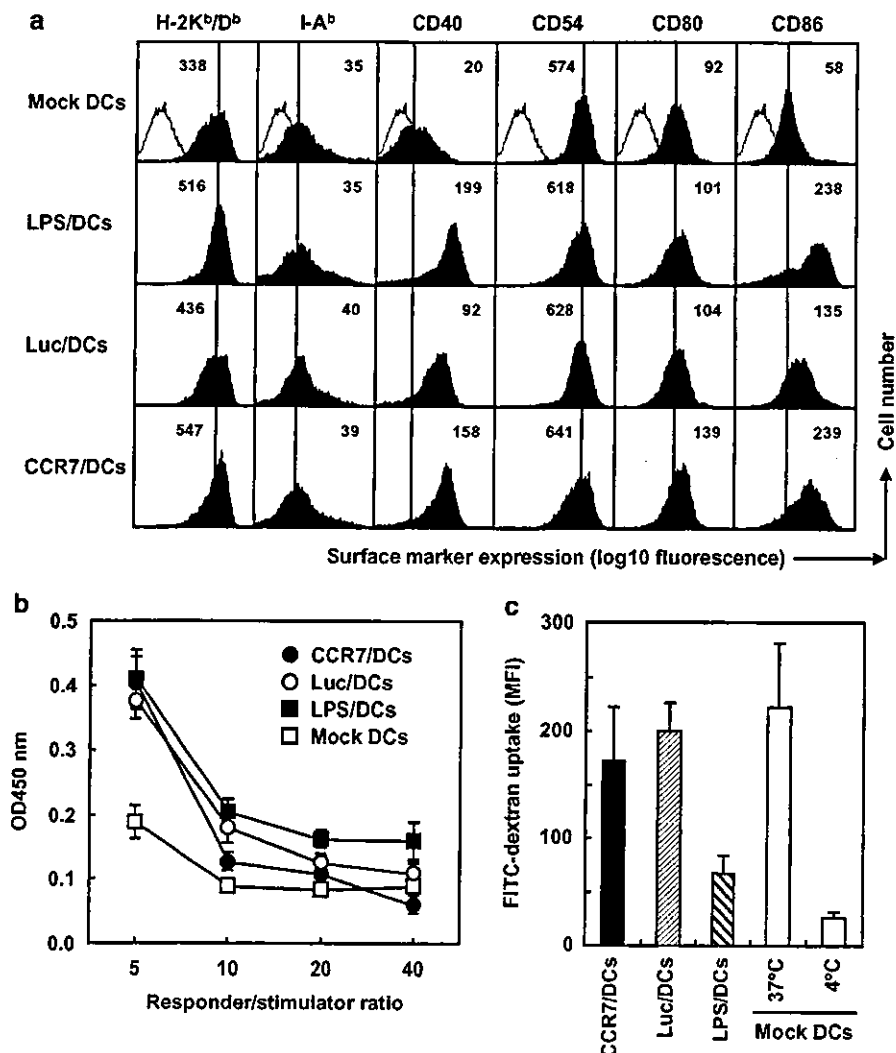

Figure 2 *Chemotactic activity of CCR7/DCs in response to CCL21. DCs were transduced with AdRGD-CCR7 or AdRGD-Luc at 50 MOI (a) or the indicated MOI (b). These transduced cells, LPS-stimulated DCs, and mock DCs were cultured for 24 h in GM-CSF-free medium. In vitro chemotaxis assay was performed by a Chemotaxicell-24 installed on a 24-well culture plate. CCL21 solution was added in the lower compartment at the indicated concentration, and DCs were placed in the upper chamber at 10^5 cells. After 4 h incubation, the number of cells that migrated to the lower compartment was counted on a NucleoCounter. Data are presented as mean ±s.d. of four independent cultures.*

Taken together, these results demonstrate that gene transduction using AdRGD-CCR7 did not eliminate the antigen-presenting cell (APC) function of DCs; rather, CCR7/DCs acquired an immunophenotype similar to mature DCs while maintaining high endocytotic capacity. Additionally, these immunological characteristics of CCR7/DCs were similar at 48 h post-transduction (data not shown).

Accumulation of CCR7/DCs in regional LN

DCs derived from enhanced green fluorescent protein-transgenic (EGFP-Tg) mice were transduced with AdRGD-CCR7 or AdRGD-Luc at 50 MOI and then cultured for 24 h. These EGFP-positive CCR7/DCs, Luc/DCs, and mock DCs were intradermally injected into the flank of wild-type mice, and their accumulation in the draining inguinal LN was compared at 48 h post-administration by flow cytometric analysis (Figure 4). In all mice, the EGFP-positive DCs were not detected in the inguinal LNs contralateral to the DC-administration site (data not shown). More than double the number of EGFP-positive DCs was detected in regional LN cells prepared from mice injected with Luc/DCs, as compared

Figure 3 Immunological characteristics of CCR7/DCs. C57BL/6 DCs were transduced with AdRGD-CCR7 or AdRGD-Luc at 50 MOI, and then were cultured for 24 h. (a) These transduced cells, LPS-stimulated DCs, and mock DCs were stained by indirect immunofluorescence using monoclonal antibodies of the indicated specificities (solid histogram). Dotted histograms represent cells stained by phycoerythrin-conjugated streptavidin alone. Values indicated in the upper part of each panel represent MFI of flow cytometric analysis. The data are representative of three independent experiments. (b) Naïve BALB/c T lymphocytes were co-cultured with CCR7/DCs, Luc/DCs, LPS/DCs, or mock DCs at the indicated responder/stimulator ratio for 3 days. Cell cultures were pulsed with BrdU during the last 18 h, and then T-cell proliferation was assessed by BrdU-ELISA. Results are expressed as mean±s.e. of three independent cultures using T cells prepared from three individual mice. (c) CCR7/DCs, Luc/DCs, LPS/DCs, and mock DCs were incubated with PBS containing 1 mg/ml FITC-dextran at 4 or 37°C. After 1 h, cells were washed five times with ice-cold PBS and uptake of FITC-dextran was assessed by flow cytometry. MFI of the flow cytometric analysis is presented in the bar chart. Data are presented as the mean±s.d. of four independent cultures.

with the mock DC-treated group. This phenomenon probably reflected the maturation status of Luc/DCs as shown in Figure 3a and b. Importantly, CCR7/DCs could migrate approximately 5.5- and 15-fold more efficiently into the regional LN than Luc/DCs and mock DCs, respectively, clearly demonstrating that CCR7 gene transduction using AdRGD was useful technology to accelerate the accumulation of DC vaccine in regional LN.

## Vaccine efficacy of DCs co-transduced with antigen and CCR7

In order to evaluate the potency of CCR7/DCs as vaccine carriers, we prepared the DC vaccine co-transduced with CCR7 gene and ovalbumin (OVA), model antigen, gene using AdRGD. As shown in Figure 5, DCs combined

with AdRGD-OVA and AdRGD-CCR7 could present OVA peptides via MHC class I molecules at levels equal to DCs transduced with AdRGD-OVA alone. On the other hand, the OVA-presentation level in DCs co-transduced with AdRGD-OVA and AdRGD-Luc decreased by half. These data revealed that CCR7 gene transduction did not affect the MHC class I-presentation pathway for antigens endogenously and simultaneously expressed in DCs, and suggested that the proteins accumulating in the cytoplasm and the membrane-localized receptors, such as luciferase and CCR7, respectively, might induce different methods for processing co-expressed endogenous antigens in DCs.

We compared the antitumor effects of DCs co-transduced with gp100, a melanoma-associated antigen, and CCR7 (gp100+CCR7/DCs) and DCs transduced with AdRGD-gp100 alone (gp100/DCs) in the murine
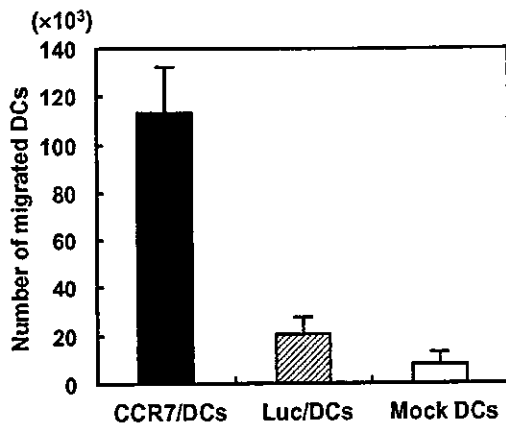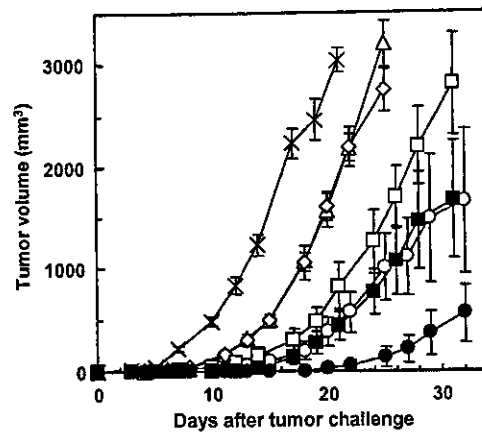
Figure 4 Migration of CCR7/DCs from administration site to draining LN. EGFP-Tg DCs were transduced with AdRGD-CCR7 or AdRGD-Luc at 50 MOI, and then were cultured for 24 h. These transduced cells and mock DCs were intradermally injected into the left flank of C57BL/6 mice at 2×10^6 cells/50 μl. After 2 days, the draining inguinal LNs were collected from these mice, and a single-cell suspension was prepared and stained by indirect immunofluorescence using anti-CD11c monoclonal antibody. The abundance of EGFP⁺CD11c⁺ DCs was assessed by flow cytometric analysis acquiring 500 000 events. The number of DCs that had migrated into draining LNs was calculated by multiplying the EGFP⁺CD11c⁺ DC frequency by the total number of isolated LN cells. Data are presented as mean±s.e. of results from four mice.
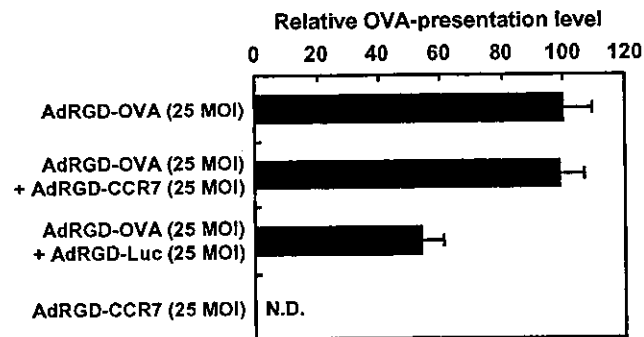
Figure 5 Antigen presentation on MHC class I molecules by CCR7/DCs. DCs were transduced with the indicated combination of AdRGD-OVA, AdRGD-CCR7, and AdRGD-Luc. These cells were co-cultured with CD8-OVA 1.3 cells for 20 h. IL-2 levels released from stimulated CD8-OVA 1.3 cells into culture supernatants were determined by ELISA, and relative OVA-presentation level via MHC class I molecules in each transduced DC was expressed as a percentage of the group using DCs transduced with AdRGD-OVA alone. Data represent the mean±s.d. of three independent cultures. ND: IL-2 secreted from CD8-OVA 1.3 cells was not detectable.

B16BL6 melanoma model. Obvious growth suppression of B16BL6 tumor challenge was achieved in mice vaccinated with gp100/DCs, as shown in our previous report,[14] whereas immunization with mock DCs or CCR7/DCs was not effective (Figure 6). This vaccine efficacy of gp100/DCs depended on the administered DC dosage. Notably, equal antitumor effects were observed in groups vaccinated with 2×10^5 gp100+CCR7/DCs and with 5×10^5 gp100/DCs, and vaccination with 5×10^5 gp100+CCR7/DCs caused extensive inhibition of B16BL6 tumor growth. Thus, we assessed B16BL6-specific CTL activity in mice vaccinated with gp100+CCR7/DCs or gp100/DCs by europium


X PBS

Δ Mock DCs (5×10^5 cells/mouse)

◇ CCR7/DCs (5×10^5 cells/mouse)

○ gp100/DCs (5×10^5 cells/mouse)

□ gp100/DCs (2×10^5 cells/mouse)

● gp100+CCR7/DCs (5×10^5 cells/mouse)

■ gp100+CCR7/DCs (2×10^5 cells/mouse)

Figure 6 Vaccine efficacy of DCs co-transduced with CCR7 and gp100 gene against B16BL6 melanoma challenge. CCR7/DCs, gp100/DCs, and gp100+CCR7/DCs were prepared using corresponding vectors at 25 MOI, and then cultured for 24 h. C57BL/6 mice were immunized by intradermal injection of transduced DCs into the left flank at the indicated cell dosage, and then 4×10^5 B16BL6 melanoma cells were inoculated into the right flank of the mice at 1 week post-vaccination. The tumor sizes were assessed using microcalipers three times per week. Each point represents the mean±s.e. of 5–10 mice.

(Eu)-release assay (Figure 7a). The effector cells prepared from mice vaccinated with gp100/DCs could strongly injure B16BL6 cells, as we reported previously.[14] In addition, the effector cells in all groups did not induce lysis of YAC-1 cells, which are highly susceptible to NK activities, and H-2 haplotype-matched irrelevant EL4 thymoma cells (data not shown). B16BL6-specific cytotoxic activity increased in splenocytes from mice vaccinated with gp100+CCR7/DCs, depending on administered DC-dosage, and cytotoxicity exceeded that observed in the group treated with gp100/DCs at same dosage (5×10^5 cells/mouse). Furthermore, re-stimulated splenocytes from mice vaccinated with gp100+CCR7/DCs at 2 or 5×10^5 cells/mouse exhibited higher frequency of interferon-γ (IFN-γ)-producing cells in ELISPOT assay in comparison with those from 5×10^5 gp100/DCs-immunized mice (Figure 7b). Taken together, these data indicated that the induction of a TAA-specific immune response can be potentiated by the improved migration of TAA-loaded DC vaccine from the administration site to lymphoid tissue.

Discussion

The development of a vaccine for cancer treatment aims for sufficient induction of the tumor-specific immune response, in which antitumor CTLs play a central role, to a level capable of tumor rejection and regression. The

134

a

b
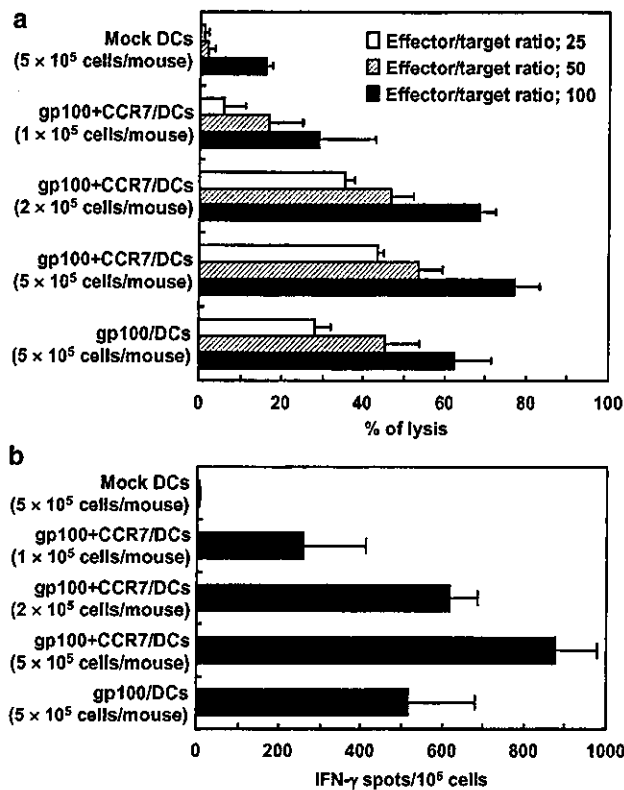
Figure 7 CTL activity and the frequency of IFN-γ-producing cells in splenocytes from mice immunized with DCs cotransduced with CCR7 and gp100 gene by AdRGD. gp100/DCs and gp100+CCR7/DCs were prepared using corresponding vectors at 25 MOI, and then cultured for 24 h. These transduced cells and mock DCs were vaccinated once intradermally into C57BL/6 mice at the indicated cell dosage. At 1 week after immunization, nonadherent splenocytes were prepared from these mice, and then were re-stimulated in vitro for 5 days with IFN-γ-stimulated and MMC-inactivated B16BL6 cells. (a) A cytolytic assay using the re-stimulated splenocytes (effector cells) was performed against IFN-γ-stimulated B16BL6 cells (target cells). The data represent the mean±s.e. of four independent cultures from four individual mice. (b) IFN-γ-producing cells in re-stimulated splenocytes were evaluated by mouse IFN-γ ELISPOT assay. The data represent the mean±s.d. of results from four mice.

efficient priming and subsequent activation of antitumor CTLs requires the processing and presentation of TAAs as peptide fragments in the context of appropriate MHC class I molecules by APCs.[15] DCs are the most potent APCs and are uniquely capable of presenting novel antigens to naive T cells to initiate and modulate immune responses.[5–7] Owing to these properties, TAA-loaded DCs are considered promising vaccine carriers in immune intervention strategies against cancer. However, very few DCs in currently available DC-based immunotherapies are capable of migrating from an adminis-tration site to regional lymphoid tissue,[16–18] where they present MHC class I- and II-restricted peptides to naive T cells, because optimal DC conditioning for enhancing migratory ability is not yet established. Therefore, increasing the migratory ability of a DC vaccine toward lymphoid tissues would remarkably improve the efficacy of DC-based immunotherapy because priming/activation of immune effector cells would be significantly promoted. In the present study, we focused on the chemokine receptor, CCR7, which manages facilitated DC migration to lymphoid tissues, and attempted to

create a DC vaccine that sufficiently expressed CCR7 on the surface by gene transduction.

A vector system that can effectively deliver a foreign gene to DCs is essential for preparing a genetically modified-DC vaccine. We have demonstrated that AdRGD can enhance gene transduction efficiency against murine and human DCs as compared with conventional Ad because of the expression of the RGD sequence, the αv-integrin-targeting peptide, at the HI loop in the fiber knob.[11–14] Therefore, we constructed AdRGD-CCR7, which carried the expression cassette containing mouse CCR7 cDNA under the control of the cytomegalovirus promoter, and confirmed the vector's performance. RT-PCR analysis indicated that transfection using AdRGD-CCR7 allowed murine bone marrow-derived DCs to express abundant CCR7 mRNA, and CCR7 mRNA expression in CCR7/DCs was the highest at 24 h after gene transduction. Furthermore, CCR7/DCs cultured for 24 h exhibited sufficient CCR7 protein expression on the cell surface in flow cytometric analysis and demonstrated strong migratory ability toward CCL21, a CCR7 ligand secreted constitutively from lymphoid tissues, depending on both CCL21 concentration in a 4 h chemotaxis assay and AdRGD-CCR7 dose in transfection. That is, efficient CCR7-gene transduction into DCs by AdRGD reinforced surface expression of CCR7, which sensed a CCL21 concentration gradient and transmitted intracellular signals associated with migration in their original biologically active form. Although DCs generally enhance the expression of CCR7 and acquire migratory ability to lymphoid tissues by various maturation stimuli, an increase in CCR7 mRNA levels and enhancement of migratory activity toward CCL21 were not observed in LPS/DCs, contrary to our expectation. Granucci et al[19] reported that DCs stimulated with LPS significantly decreased their intrinsic migratory ability and increased the antigen uptake function at 1–2 h post-stimulation. This phenomenon probably represents the in vivo stage during which DCs remain at an inflammation site caused by the components of invading bacteria, such as LPS, and capture antigens by full endocytosis. In addition, Granucci et al[19] demonstrated that, at around 4 h after LPS activation, DCs recovered their migratory ability and started to progressively lose antigen uptake function until they reached the mature stage in which LPS/DCs showed poor antigen uptake and migratory activity. Therefore, because in the present study we tested the responses 24 h after LPS stimulation, low CCR7 mRNA levels and poor migratory response to CCL21 by LPS/DCs may have been observed because tests were run after the optimal time point, suggesting that the control of DC-migratory activity by LPS stimulation is difficult.

DCs are strong initiators of defense mechanisms that combat infectious diseases and cancer, but, in their role as APCs, DCs are also involved in immune suppression and immune tolerance.[20–23] In their induction of a positive immune response, immature DCs capture invading antigens at peripheral locations and are then activated by inflammatory stimuli, such as interleukin (IL)-1β, tumor necrosis factor-α, and bacterial components, to migrate to T-cell-rich areas in regional LN. In these processes, DCs enhance the expression of MHC/costimulatory molecules, which is essential for T-cell surface sensitization for effective induction of T-cell-

dependent primary immune responses. On the other hand, in negative immune regulation, immature DCs take up resident biological materials or apoptotic bodies and present processing peptides without acquiring activated phenotypes during migration to regional LN.[24,25] Therefore, a full analysis and understanding of immunological characteristics of DC vaccine is imperative for the development of DC-based immunotherapy because the polarity of the immune response is greatly influenced by the activated state of DCs during T-cell sensitization. CCR7/DCs created in the present study maintained inherent endocytotic activity, suggesting that CCR7/DCs administered into tumor tissue can capture necrotic or apoptotic tumor cell fragments and may induce TAA-specific immune responses. Yanagawa et al[26] reported that internalization of FITC-dextran in murine mature DCs increased in the presence of CCR7 ligand, CCL19 or CCL21. These results support the notion that CCL21, secreted from lymphatic vessels located near a tumor, may encourage uptake of tumor cell fragments by CCR7/DCs injected into the tumor tissue. Although high endocytotic activity is a characteristic feature of immature DCs, flow cytometric analysis indicated that CCR7/DCs enhanced expression of MHC/costimulatory molecules and allo-MLR suggested the reinforcement of T-cell proliferation-stimulating ability. These results agreed with our previous report demonstrating that transduction using AdRGD could enhance the maturation status of DCs,[13] strongly suggesting that CCR7 gene transduction using AdRGD did not inhibit the original APC characteristics of DCs and that CCR7/DCs can function as a useful vaccine possessing sufficient T-cell activation ability in vivo.

Although a technique to label DCs with radioisotopes or fluorescent substances is frequently used for evaluating in vivo kinetics of administered DC vaccines,[27-32] release via exosomes or leakage of the labeling material from DCs complicates the analysis. Eggert et al[33] reported that application of EGFP-Tg mouse-derived DCs avoided this problem and enabled simple evaluation and analysis of the kinetics of administered DCs without the need for labeling. Thus, we investigated the migratory ability of CCR7/DCs by flow cytometric analysis of regional LN cells prepared from mice intradermally injected with transduced EGFP-Tg mouse-derived DCs. At 48 h post-injection, regional LNs that served as administration sites for CCR7/DCs were obviously larger than contralateral LNs under macroscopic observation, and the frequency of EGFP+CD11c+ DCs in regional LN cells was 1.93 ± 0.54, 0.57 ± 0.19, and 0.12 ± 0.04% (mean ± s.e.) for CCR7/DCs-, Luc/DCs-, and mock DCs-injected mice, respectively. In addition, we could prepare more cells from regional LN in CCR7/DCs-injected mice than from the Luc/DC or mock DC groups, suggesting that not only administered DCs but also other immune cells, such as T cells, might accumulate in regional LN in mice injected with CCR7/DCs.

Previously, we demonstrated that immunization with DCs efficiently transduced with gp100 gene by AdRGD could significantly inhibit the growth and lung metastasis of murine B16BL6 melanoma in vivo.[14] In order to actually evaluate the predominancy of CCR7-transduced DCs as a vaccine carrier in vivo, we investigated anti-B16BL6 melanoma effects in mice vaccinated with DCs genetically engineered to simultaneously express gp100

and CCR7. Although antigen presentation via MHC class I molecules in the experiment using AdRGD-OVA was the same for DCs transduced with OVA gene alone and co-transduced with OVA and CCR7 gene, immunization with gp100+CCR7/DCs could more effectively suppress growth of B16BL6 tumors than vaccination with gp100/DCs. Furthermore, DC vaccine co-transduced with the TAA gene and the CCR7 gene effectively induced TAA-specific and IFN-γ-producing CTLs using a lower dosage than conventional DC vaccine transduced with TAA gene alone. These data suggest that augmentation of lymphoid tissue directivity of DCs by efficient CCR7-gene transduction can reduce the DC vaccine dosage that is needed to elicit efficacious therapeutic effects in DC-based immunotherapy. In other words, this method may considerably reduce the cost, time, and effort for DC vaccine preparation and relieve the patient from the burden of frequent blood drawing for DC isolation.

In conclusion, our data strongly suggested that in vivo kinetic control of DC vaccine, namely the establishment of an active DC delivery system to lymphoid tissues, was very useful for improving the efficacy of DC-based immunotherapy. We expect that superior lymphoid tissue accumulation of DCs transduced with the CCR7 gene is advantageous for a vaccine carrier because of efficient activation of immune effector cells in regional LNs and a rapid supply of activated effector cells to the whole body. Recently, optimized DC conditioning, which includes stimulation of antigen-presenting DCs with various cytokines or ligand molecules, has been investigated for the development of more effective DC-based immunotherapy. Several reports demonstrated that DC stimulation by prostaglandin E2[34-36] or the pre-induction of inflammatory response at the DC-administration site[37] was effective in promoting migration of administered DCs to lymphoid tissues. Further research and development of 'lymphoid tissue-directivity DC' vaccine based on these data and our results may greatly improve efficacy and lead to clinical application of DC-based immunotherapy.

Materials and methods

Cell lines and mice
A murine B16BL6 melanoma cell line (H-2[b]) was cultured in minimum essential medium supplemented with 7.5% fetal bovine serum (FBS) and antibiotics. The helper cell line, 293 cells, was grown in Dulbecco's modified Eagle medium supplemented with 10% FBS and antibiotics. CD8-OVA 1.3 cells,[38] specific T–T hybridoma against OVA+ H-2K[b] (kindly provided by Dr CV Harding; Department of Pathology, Case Western Reserve University, Cleveland, OH, USA), were maintained in Dulbecco's modified Eagle medium supplemented with 10% FBS, 50 μM 2-mercaptoethanol, and antibiotics. Female C57BL/6 mice (H-2[b]) and female BALB/c mice (H-2[d]), aged 7–8 weeks, were purchased from SLC Inc. (Hamamatsu, Japan). EGFP-Tg mice, C57BL/6 TgN(act-EGFP)OsbC14-Y01-FM131,[39] were kindly provided by Dr M Okabe (Genome Information Research Center, Osaka University, Suita, Japan). All mice were held under specific pathogen-free conditions and the experimental procedures were in accordance with the Osaka University guidelines for the welfare of animals in experimental neoplasia.

Vectors

Replication-deficient AdRGD was based on the adenovirus serotype 5 backbone with deletions of E1 and E3 regions. The RGD sequence for αv-integrin targeting was inserted into the HI loop of the fiber knob using a two-step method as described previously.[40] The expression cassette containing mouse CCR7 cDNA derived from pBluescript SK(+)/mCCR7 under the control of the cytomegalovirus promoter was inserted into the E1-deletion site to construct AdRGD-CCR7, using an improved *in vitro* ligation method as described previously.[40–42] Luciferase-expressing AdRGD (AdRGD-Luc), OVA-expressing AdRGD (AdRGD-OVA), and gp100-expressing AdRGD (AdRGD-gp100) were constructed previously.[12–14] All recombinant AdRGDs were propagated in 293 cells, purified by two rounds of cesium chloride gradient ultracentrifugation, dialyzed, and stored at −80°C. Titers of infective AdRGD particles were evaluated by the end-point dilution method using 293 cells.

Mouse bone marrow-derived DCs

DCs were prepared according to the method of Lutz *et al*,[43] with slight modification. Briefly, bone marrow cells flushed from the femurs and tibias of C57BL/6 or EGFP-Tg mice were seeded at 5×10^6 cells per sterile 100-mm bacterial grade culture dish in 10 ml of RPMI 1640 containing 10% FBS, 40 ng/ml recombinant murine granulocyte/macrophage colony-stimulating factor (GM-CSF; kindly provided by KIRIN Brewery Co., Ltd, Tokyo, Japan), 50 μM 2-mercaptoethanol, and antibiotics. On day 3, another 10 ml of culture medium was added to the dish for medium replenishment. On day 6, 10 ml of the culture supernatant was collected and centrifuged at 1500 rpm for 5 min at room temperature, and the pellet was resuspended in 10 ml of fresh culture medium, and then returned to the original dish to conserve unattached cells. Eight-day-old DCs (nonadherent cells) were harvested and used as intact immature DCs in subsequent experiments. DCs cultured for another 24 h with media containing 1 μg/ml LPS (Nacalai Tesque, Inc., Kyoto, Japan) were used as phenotypically mature DCs.

Viral transduction into DCs

DCs were suspended at a concentration of 5×10^6 cells/ml in FBS-free RPMI 1640 and placed in a 15-ml conical tube. Each AdRGD was added at various MOI, the suspension was mixed well, and the tube was incubated at 37°C for 2 h with occasional gentle agitation. The cells were washed three times with phosphate-buffered saline (PBS) and resuspended in a suitable solution.

Semiquantitative RT-PCR analysis

CCR7/DCs, Luc/DCs, and mock DCs were cultured on 100-mm bacterial grade culture dishes in GM-CSF-free culture medium. Mouse CCR7 gene expression was assessed by semiquantitative RT-PCR analysis as follows. Total RNA was isolated from these cells and LPS/DCs using Sepasol-RNA I Super (Nacalai Tesque, Inc.) according to the manufacturer's instructions, and then RT proceeded for 60 min at 42°C in a 50 μl reaction mixture containing 5 μg total RNA treated with DNase I, 10 μl 5× RT buffer, 5 mM $MgCl_2$, 1 mM dNTP mix, 1 μM random primer (9-mer), 1 μM oligo(dT)$_{20}$, and 100 U

ReverTra Ace (TOYOBO Co., Ltd, Osaka, Japan). PCR amplification of the CCR7 and β-actin transcripts was performed in 50 μl of a reaction mixture containing 1 μl of RT material, 5 μl 10 × PCR buffer, 1.25 U *Taq* DNA polymerase (TOYOBO Co., Ltd), 1.5 mM $MgCl_2$, 0.2 mM dNTP, and 0.4 μM primers. The sequences of the specific primers were as follows; mouse CCR7: forward, 5′-aca gcg gcc tcc aga aga aca gcg g-3′; reverse, 5′-tga cgt cat agg caa tgt tga gct g-3′; mouse β-actin: forward, 5′-tgt gat ggt ggg aat ggg tca g-3′; reverse, 5′-ttt gat gtc acg cac gat ttc c-3′. After denaturation for 2 min at 95°C, 20 cycles of denaturation for 30 s at 95°C, annealing for 30 s at 60°C, and extension for 30 s at 72°C were repeated and followed by completion for 4 min at 72°C. The PCR product was electrophoresed through a 3% agarose gel, stained with ethidium bromide, and visualized under UV radiation. The expected PCR product sizes were 345 bp (CCR7) and 514 bp (β-actin). Quantification of PCR products was performed by densitometry analysis, and the relative CCR7 mRNA expression level was calculated as the ratio of the densitometric units of CCR7 PCR-products to the densitometric units of β-actin PCR products.

Flow cytometric analysis for mouse CCR7

CCR7/DCs and Luc/DCs were prepared by using corresponding vectors at 50 MOI. These transduced DCs, LPS/DCs, and mock DCs were cultured on 100-mm bacterial grade culture dishes in GM-CSF-free culture medium for 24 h. The cells (1×10^6) were fixed by incubation for 10 min in 2% paraformaldehyde, and then incubated with 100 μl staining buffer (PBS containing 0.1% bovine serum albumin and 0.01% NaN_3) containing the anti-FcγRII/III monoclonal antibody (2.4G2; rat $IgG_{2b,κ}$; BD Biosciences, San Jose, CA, USA) to block nonspecific binding of the subsequently used antibody reagents. After 1 h, the cells were incubated overnight with anti-mouse CCR7 polyclonal antibody (goat Ig; ImmunoDetect Inc., Fayetteville, NY, USA) at a 1:10 dilution. Successively, cells were incubated for 2 h with FITC-conjugated rabbit anti-goat Ig (DakoCytomation, Kyoto, Japan) at a 1:100 dilution. Finally, 30 000 events of the stained cells were analyzed for mouse CCR7 protein expression by a FACSCalibur flow cytometer using CellQuest software (Becton Dickinson, Tokyo, Japan). Between all incubation steps, cells were washed three times with staining buffer.

In vitro chemotaxis assay

CCR7/DCs, Luc/DCs, and mock DCs were cultured for 24 or 48 h in GM-CSF-free medium. Chemotactic activity of these DCs and LPS/DCs for CCL21 was measured by an *in vitro* chemotaxis assay across a polycarbonate membrane with 5-μm pores (Chemotaxicell-24; Kurabo Industries Ltd, Osaka, Japan). Recombinant murine CCL21 (PeproTech EC Ltd, London, England) dissolved in an assay medium (RPMI 1640 containing 0.5% bovine serum albumin and 20 mM HEPES) was added to a 24-well culture plate. DCs were suspended with the assay medium and were placed in a Chemotaxicell-24 installed on each well at 10^6 cells. Cell migration was allowed for 4 h at 37°C in a 5% CO_2 atmosphere. Cells that migrated into the lower compartment were counted using a NucleoCounter™ (ChemoMetec, Allerød, Denmark), and the chemotactic activity was expressed in terms of

the percentage of the input cells calculated by the following formula: (% of input cells) = (the number of migrated cells)/(the number of cells placed in Chemotaxicell-24; 10^6 cells) × 100.

Analysis of surface marker expression

All immunoreagents used in this experiment were purchased from BD Biosciences. CCR7/DCs and Luc/DCs were prepared by using corresponding vectors at 50 MOI. At 24 h after transduction, immunophenotype of transduced DCs, LPS/DCs, and mock DCs was confirmed by flow cytometric analysis. Briefly, 10^6 cells in 100 µl staining buffer were incubated for 30 min on ice with the 2.4G2 monoclonal antibody to block nonspecific binding of the subsequently used immunoreagents. The cells were resuspended in 100 µl staining buffer and incubated for 30 min on ice using the manufacturer's recommended amounts of biotinylated monoclonal antibodies: 28-8-6 (anti-H-2K^b/D^b), AF6-120.1 (anti-I-A^b), 3/23 (anti-CD40), 3E2 (anti-CD54), 16-10A1 (anti-CD80), and GL1 (anti-CD86). The cells were then resuspended in 100 µl staining buffer containing phycoerythrin-conjugated streptavidin at a 1:200 dilution, and nonspecific binding was measured using phycoerythrin-conjugated streptavidin alone. After incubation for 30 min on ice, 30 000 events of the stained cells were analyzed for surface phenotype by flow cytometry. Between all incubation steps, cells were washed three times with staining buffer.

Allogenic MLR

C57BL/6 DCs were transduced with AdRGD-CCR7 or AdRGD-Luc at 50 MOI, and then cultured for 24 h. Allogenic naive T cells were purified from BALB/c splenocytes as nylon wool nonadherent cells, and were used as responder cells at 1 × 10^5 cells/well in 96-well plates. CCR7/DCs, Luc/DCs, LPS/DCs, or mock DCs (stimulator cells) were inactivated by 50 µg/ml mitomycin C (MMC) for 30 min and added to responder cells in varying cell numbers. Cells were co-cultured in 100 µl RPMI 1640 supplemented with 10% FBS, 50 µM 2-mercaptoethanol, and antibiotics at 37°C and 5% CO$_2$ for 3 days. Control wells contained either stimulator cells alone or responder cells alone. Cell cultures were pulsed with 5-bromo-2'-deoxyuridine (BrdU) during the last 18 h, and then proliferation of responder cells was evaluated by Cell Proliferation ELISA, BrdU (Roche Diagnostics Co., Indianapolis, IN, USA).

Antigen uptake assay

CCR7/DCs and Luc/DCs were prepared by using corresponding vectors at 50 MOI. These cells, LPS/DCs, and mock DCs were cultured for 24 h, and then resuspended at 5 × 10^6 cells/ml in ice-cold PBS containing 1 mg/ml FITC-dextran (MW: 77 000; Sigma Chemical Co., St Louis, MO, USA). The cells were incubated at 37 or 4°C to determine background uptake. After 1 h, the cells were washed extensively with ice-cold PBS and analyzed by flow cytometry.

In vivo migration assay

EGFP-Tg mouse-derived DCs were transduced with AdRGD-CCR7 or AdRGD-Luc at 50 MOI, and then cultured for 24 h. These transduced cells and mock DCs were intradermally injected into the left flank of wild-type C57BL/6 mice at 2 × 10^6 cells/50 µl. After 2 days, the draining inguinal LNs were collected from these mice, and then a single-cell suspension was prepared. The isolated LN cells were blocked by 2.4G2 monoclonal antibody and stained by indirect immunofluorescence with biotinylated anti-CD11c monoclonal antibody (HL3; BD Biosciences) and PerCP-conjugated streptavidin. The stained cells were analyzed by flow cytometry acquiring 500 000 events, and the number of migrated DCs into draining LNs was calculated by multiplying the EGFP$^+$CD11c$^+$ cell frequency by the total number of isolated LN cells.

Antigen-presentation assay

C57BL/6 DCs were transduced with various combinations of AdRGD-OVA, AdRGD-CCR7, and AdRGD-Luc each at 25 MOI, and then seeded on a 96-well flat-bottom culture plate at a density of 1 × 10^5 cells/well. These cells were co-cultured with 1 × 10^5 cells/well CD8-OVA 1.3 cells at 37°C for 20 h. The response of stimulated CD8-OVA 1.3 cells was assessed by determining the amount of IL-2 released into an aliquot of culture medium (100 µl) using a murine IL-2 ELISA KIT (Biosource International, Camarillo, CA, USA). Relative OVA-presentation level via MHC class I molecules in each transduced DC was calculated by the following formula: (relative OVA-presentation level) = (IL-2 level in tested group)/(IL-2 level in group using DCs transduced with AdRGD-OVA alone) × 100.

Tumor protection assay

DCs were transduced with AdRGD-CCR7 alone, AdRGD-gp100 alone, or a combination of AdRGD-CCR7 and AdRGD-gp100, each at 25 MOI, and then cultured for 24 h. These transduced DCs and mock DCs were intradermally injected into the left flank of C57BL/6 mice at 2 or 5 × 10^5 cells/50 µl. At 1 week after the vaccination, 4 × 10^5 B16BL6 melanoma cells were intradermally inoculated into the right flank of the mice. The major and minor axes of the tumor were measured using microcalipers, and the tumor volume was calculated by the following formula: (tumor volume; mm^3) = (major axis; mm) × (minor axis; mm)^2 × 0.5236. The mice were euthanized when one of the two measurements was greater than 20 mm.

Eu-release assay and ELISPOT assay for B16BL6-specific CTLs

DCs were transduced with AdRGD-gp100 alone or a combination of AdRGD-CCR7 and AdRGD-gp100 at 25 MOI, and then cultured for 24 h. These transduced DCs and mock DCs were administered once intradermally into the left flank of C57BL/6 mice at 1, 2, or 5 × 10^5 cells/50 µl. At 1 week after immunization, nonadherent splenocytes were prepared from these mice and re-stimulated in vitro using B16BL6 cells, which were cultured in media containing 100 U/ml recombinant murine IFN-γ (PeproTech EC Ltd) for 24 h and inactivated with 50 µg/ml MMC at 37°C for 30 min, at an effector/stimulator ratio of 10 in RPMI 1640 supplemented with 10% FBS, 50 µM 2-mercaptoethanol, and antibiotics. After 5 days, the splenocytes were collected and used as CTL effector cells. Target cells, IFN-γ-stimulated B16BL6 cells, were Eu-labeled and a Eu-release assay

138

was performed as described previously.[44] Cytolytic activity was determined using the following formula: (% of lysis) = ((experimental Eu release—spontaneous Eu release)/(maximum Eu release—spontaneous Eu release)) × 100. Spontaneous Eu release of the target cells was <10% of maximum Eu release by the detergent. In addition, IFN-γ-producing cells in the re-stimulated splenocytes were detected by using Mouse IFN-γ ELISPOT Kit (BD Biosciences) according to the manufacturer's instruction. Splenocytes from unimmunized mice had a frequency of three IFN-γ spots/10^6 cells with or without re-stimulation.

Acknowledgements

References

1 Nestle FO et al. Vaccination of melanoma patients with peptide- or tumor lysate-pulsed dendritic cells. Nat Med 1998; 4: 328–332.

2 Thurner B et al. Vaccination with Mage-3A1 peptide-pulsed mature, monocyte-derived dendritic cells expands specific cytotoxic T cells and induces regression of some metastases in advanced stage IV melanoma. J Exp Med 1999; 190: 1669–1678.

3 Lodge PA et al. Dendritic cell-based immunotherapy of prostate cancer: immune monitoring of a phase II clinical trial. Cancer Res 2000; 60: 829–833.

4 Yu JS et al. Vaccination of malignant glioma patients with peptide-pulsed dendritic cells elicits systemic cytotoxicity and intracranial T-cell infiltration. Cancer Res 2001; 61: 842–847.

5 Banchereau J, Steinman RM. Dendritic cells and the control of immunity. Nature 1998; 392: 245–252.

6 Steinman RM et al. Antigen capture, processing, and presentation by dendritic cells: recent cell biological studies. Hum Immunol 1999; 60: 562–567.

7 Mellman I, Steinman RM. Dendritic cells: specialized and regulated antigen processing machines. Cell 2001; 106: 255–258.

8 Gunn MD et al. Mice lacking expression of secondary lymphoid organ chemokine have defects in lymphocyte homing and dendritic cell localization. J Exp Med 1999; 189: 451–460.

9 Förster R et al. CCR7 coordinates the primary immune response by establishing functional microenvironments in secondary lymphoid organs. Cell 1999; 99: 23–33.

10 Arthur JF et al. A comparison of gene transfer methods in human dendritic cells. Cancer Gene Ther 1997; 4: 17–25.

11 Okada N et al. Efficient gene delivery into dendritic cells by fiber-mutant adenovirus vectors. Biochem Biophys Res Commun 2001; 282: 173–179.

12 Okada N et al. Efficient antigen gene transduction using Arg-Gly–Asp fiber-mutant adenovirus vectors can potentiate antitumor vaccine efficacy and maturation of murine dendritic cells. Cancer Res 2001; 61: 7913–7919.

13 Okada N et al. Gene transduction efficiency and maturation status in mouse bone marrow-derived dendritic cells infected with conventional or RGD fiber-mutant adenovirus vectors. Cancer Gene Ther 2003; 10: 421–431.

14 Okada N et al. Dendritic cells transduced with gp100 gene by RGD fiber-mutant adenovirus vectors are highly efficacious in generating anti-B16BL6 melanoma immunity in mice. Gene Therapy 2003; 10: 1891–1902.

15 Lanzavecchia A. Identifying strategies for immune intervention. Science 1993; 260: 937–944.

16 Lappin MB et al. Analysis of mouse dendritic cell migration in vivo upon subcutaneous and intravenous injection. Immunology 1999; 98: 181–188.

17 Martín-Fontecha A et al. Regulation of dendritic cell migration to the draining lymph node: impact on T lymphocyte traffic and priming. J Exp Med 2003; 198: 615–621.

18 Kleindienst P, Brocker T. Endogenous dendritic cells are required for amplification of T cell responses induced by dendritic cell vaccines in vivo. J Immunol 2003; 170: 2817–2823.

19 Granucci F et al. Early events in dendritic cell maturation induced by LPS. Microbes Infect 1999; 1: 1079–1084.

20 Dhodapkar MV et al. Antigen-specific inhibition of effector T cell function in human after injection of immature dendritic cells. J Exp Med 2001; 193: 233–238.

21 Steinman RM, Nussenzweig MC. Avoiding horror autotoxicus: the importance of dendritic cells in peripheral T cell tolerance. Proc Natl Acad Sci USA 2002; 99: 351–358.

22 Steinbrink K et al. CD4+ and CD8+ anergic T cells induced by interleukin-10-treated human dendritic cells display antigen-specific suppressor activity. Blood 2002; 99: 2468–2476.

23 Mahnke K et al. Immature, but not inactive: the tolerogenic function of immature dendritic cells. Immunol Cell Biol 2002; 80: 477–483.

24 Huang FP et al. A discrete subpopulation of dendritic cells transports apoptotic intestinal epithelial cells to T cell areas of mesenteric lymph nodes. J Exp Med 2000; 191: 435–444.

25 Hemmi H et al. Skin antigens in the steady state are trafficked to regional lymph nodes by transforming growth factor-β1-dependent cells. Int Immunol 2001; 13: 695–704.

26 Yanagawa Y, Onoe K. CCR7 ligands induce rapid endocytosis in mature dendritic cells with concomitant up-regulation of Cdc42 and Rac activities. Blood 2003; 101: 4923–4929.

27 Saeki H, Moore AM, Brown MJ, Hwang ST. Secondary lymphoid-tissue chemokine (SLC) and CC chemokine receptor 7 (CCR7) participate in the emigration pathway of mature dendritic cells from the skin to regional lymph nodes. J Immunol 1999; 162: 2472–2475.

28 Curiel-Lewandrowski C et al. Transfection of immature murine bone marrow-derived dendritic cells with the granulocyte-macropharge colony-stimulating factor gene potently enhances their in vivo antigen-presenting capacity. J Immunol 1999; 163: 174–183.

29 Hirao M et al. CC chemokine receptor-7 on dendritic cell is induced after interaction with apoptotic tumor cells: critical role in migration from the tumor site to draining lymph nodes. Cancer Res 2000; 60: 2209–2217.

30 Wu MT, Hwang ST. CXCR5-transduced bone marrow-derived dendritic cells traffic to B cell zones of lymph nodes and modify antigen-specific immune responses. J Immunol 2002; 168: 5096–5102.

31 Nakamura M et al. Dendritic cells genetically engineered to simultaneously express endogenous tumor antigen and

granulocyte macrophage colony-stimulating factor elicit potent therapeutic antitumor immunity. *Clin Cancer Res* 2002; **8**: 2742–2749.

32 de Vries IJM *et al.* Effective migration of antigen-pulsed dendritic cells to lymph nodes in melanoma patients is determined by their maturation state. *Cancer Res* 2003; **63**: 12–17.

33 Eggert AAO *et al.* Analysis of dendritic cell trafficking using EGFP-transgenic mice. *Immunol Lett* 2003; **89**: 17–24.

34 Scandella E *et al.* Prostaglandin E2 is a key factor for CCR7 surface expression and migration of monocyte-derived dendritic cells. *Blood* 2002; **100**: 1354–1361.

35 Scandella E *et al.* CCL19/CCL21-triggered signal transduction and migration of dendritic cells requires prostaglandin E2. *Blood* 2004; **103**: 1595–1601.

36 Sato M *et al.* Generation of mature dendritic cells fully capable of T helper type 1 polarization using OK-432 combined with prostaglandin E$_2$. *Cancer Sci* 2003; **94**: 1091–1098.

37 Nair S *et al.* Injection of immature dendritic cells into adjuvant-treated skin obviates the need for *ex vivo* maturation. *J Immunol* 2003; **171**: 6275–6282.

38 Pfeifer JD *et al.* Phagocytic processing of bacterial antigens for class I MHC presentation to T cells. *Nature* 1993; **361**: 359–362.

39 Okabe M *et al.* Green mice as a source of ubiquitous green cells. *FEBS Lett* 1997; **407**: 313–319.

40 Mizuguchi H *et al.* A simplified system for constructing recombinant adenoviral vectors containing heterologous peptides in the HI loop of their fiber knob. *Gene Therapy* 2001; **8**: 730–735.

41 Mizuguchi H, Kay MA. Efficient construction of a recombinant adenovirus vector by an improved *in vitro* ligation method. *Hum Gene Ther* 1998; **9**: 2577–2583.

42 Mizuguchi H, Kay MA. A simple method for constructing E1- and E1/E4-deleted recombinant adenoviral vectors. *Hum Gene Ther* 1999; **10**: 2013–2017.

43 Lutz MB *et al.* An advanced culture method for generating large quantities of highly pure dendritic cells from mouse bone marrow. *J Immunol Methods* 1999; **223**: 77–92.

44 Okada N *et al.* Administration route-dependent vaccine efficiency of murine dendritic cells pulsed with antigens. *Br J Cancer* 2001; **84**: 1564–1570.

Brief Report

Adenovirus Vector-Mediated Doxycycline-Inducible RNA Interference

TETSUJI HOSONO,[1] HIROYUKI MIZUGUCHI,[1] KAZUFUMI KATAYAMA,[2] ZHI-LI XU,[1]
FUMINORI SAKURAI,[1] AKIKO ISHII-WATABE,[3] KENJI KAWABATA,[1] TERUHIDE YAMAGUCHI,[1]
SHINSAKU NAKAGAWA,[2] TADANORI MAYUMI,[2] and TAKAO HAYAKAWA[4]

ABSTRACT

RNA interference (RNAi) is a powerful tool for the knockdown of gene expression. Here, we report on the development of an adenovirus (Ad) vector-mediated doxycycline (Dox)-inducible small interfering RNA (siRNA) expression system. We used this siRNA system to control the expression of p53 and c-Myc in human cancer cells. Coinfection of Ad vectors containing the siRNA expression system under the control of the Dox-inducible H1 promoter and Ad vectors expressing a tetracycline repressor inhibited the expression levels of p53 and c-Myc in a dose-dependent manner with both Dox and viral dose. Regulated silencing of p53 and c-Myc expression was obtained. Because an Ad vector-mediated inducible RNAi system can efficiently transduce a variety of cell types *in vitro* and *in vivo*, and the degree of loss of gene expression can be modulated according to the dose of Dox, this expression system should be a useful tool for both basic research on the analysis of gene function and therapeutic applications of RNAi.

INTRODUCTION

RNA INTERFERENCE (RNAi) mediates the sequence-specific suppression of gene expression in a wide variety of eukaryotes by double-stranded RNA homologies to the target gene (McManus and Sharp, 2002). In mammalian cells, small interfering RNA (siRNA; 19- to 29-nucleotide RNA) leads to the inhibition of target gene expression in a sequence-specific manner (Elbashir *et al.*, 2001). Vector-based siRNA systems have also been developed with RNA polymerase III (Pol III) promoters, such as the small nuclear RNA U6 promoter or the human RNase P RNA H1 promoter, to express siRNA (Brummelkamp *et al.*, 2002; Lee *et al.*, 2002; Miyagishi and Taira, 2002; Paddison *et al.*, 2002; Paul *et al.*, 2002; Sui *et al.*, 2002; Yu *et al.*, 2002). Because Pol III promoters, however, are constitutive and ubiquitous, knockdown of the target gene in an inducible or cell-specific manner is more difficult than with the

RNA polymerase II (Pol II) promoters. An inducible RNAi system becomes a more powerful tool for the analysis of gene function, because the loss-of-function or phenotype change can be analyzed according to the degree of loss of gene expression.

In the present study, we developed a doxycycline (Dox)-inducible siRNA expression system utilizing the H1 promoter containing a tetracycline operator (*tetO*) sequence. This vector system was constructed by modifying the Pol II promoter-based gene regulation system, using the tetracycline repressor (TetR), which was developed by Yao *et al.* (1998). In the absence of Dox, TetR binds the *tetO* sequence in the modified H1 promoter, thus preventing transcription. In contrast, TetR does not bind the *tetO* sequence in the presence of Dox, thus allowing transcription. Therefore, target gene expression is turned off in the absence of Dox, but is turned on in its presence.

As a delivery system for the inducible-siRNA expression cassette, the adenovirus (Ad) vector was employed because of its

numerous attractive characteristics. Recombinant Ad vector has been extensively used to deliver foreign genes to a variety of cell types and tissues both *in vitro* and *in vivo*. Ad vector can be easily grown to high titer, and can efficiently transfer genes into both dividing and nondividing cells. Furthermore, several types of improved Ad vector systems, such as tropism-modified vectors, have been developed (Curiel, 1999; Wickham, 2000; Koizumi *et al.*, 2003a,b). An Ad vector-mediated inducible siRNA expression system would be an effective strategy to use for the basic analysis of gene function and have potential for therapeutic use. In the present study, we demonstrate the efficiency of Ad vector-mediated inducible RNAi against two endogenous genes: *p53* and *c-myc*.

MATERIALS AND METHODS

Cells

293 cells were cultured with Dulbecco's modified Eagle's medium supplemented with 10% fetal calf serum (FCS). A549 cells were cultured with F12-K nutrient mixture (Kaighn's modification) medium supplemented with 10% FCS. HepG2 cells were cultured with minimum essential medium supplemented with 10% FCS.

Plasmid and virus

H1 promoter was amplified from human genomic DNA (BD Biosciences Clontech, Palo Alto, CA), using the following primers: 5'-ccatggaattcgaacgctgacgtc-3' and 5'-gcaagcttagatct-gtgtctcatacagaacttataaattccc-3'. The amplified polymerase chain reaction (PCR) product was inserted into the *Eco*RI–*Bgl*II site of pHM5 (Mizuguchi and Kay, 1999), generating pHM5-H1. H1 promoter containing the *tetO* sequence was amplified from pHM5-H1, using the following primers: 5'-tttgccagaattc-gaacgctgacgtcatcaacccg-3' and 5'-ttggaagatctctatcactgatagggа-cttataagattcccaaatccaaagacatttcacgtttatg-3' (*tetO* sequence is underlined). The amplified PCR product was inserted into the *Eco*RI–*Bgl*II site of pHM5-H1, generating pHM5-H1tetO. pHM5-H1 and pHM5-H1tetO are designed to express short hairpin RNA (shRNA) on the insertion of an appropriate sequence into the *Bgl*II–*Xba*I site. To insert the target sequence that encodes *p53* and *c-myc* shRNA, oligonucleotides for *p53* (5'-gatccccgactccagtggtaatctact<u>tcaagagag</u>tagattaccactg-gagtctttttggaaat-3' and 5'-ctagatttccaaaaagactccagtggtaatctact<u>ctttgaa</u>gtagattaccactggagtcggg-3') (Brummelkamp *et al.*, 2002) and *c-myc* (5'-gatccccgatgaggaagaaatcgat<u>gttcaagagacat</u>cgatt-tcttcctcatcttttttggaaat-3' and 5'-ctagatttccaaaaagatgaggaag-aaatcgatg<u>tctcttgaac</u>atcgatttcttcctcatcggg-3') (loop sequences are underlined) (van de Wetering *et al.*, 2003) were synthesized, annealed, and cloned into the *Bgl*II and *Xba*I sites of pHM5-H1 and pHM5-H1tetO, generating pHM5-H1-p53, pHM5-H1-Myc, pHM5-H1tetO-p53, and pHM5-H1tetO-Myc, respectively. The sequence was verified with a DNA sequencer (ABI PRISM 310; Applied Biosystems, Foster City, CA).

Ad vectors were constructed by an improved *in vitro* ligation method (Mizuguchi and Kay, 1998, 1999). Briefly, pHM5-H1-p53, pHM5-H1-Myc, pHM5-H1tetO-p53, and pHM5-H1tetO-Myc were digested with I-*Ceu*I and PI-*Sce*I, and then ligated with I-*Ceu*I- and PI-*Sce*I-digested pAdHM15-RGD

(Mizuguchi *et al.*, 2001). The resulting plasmids were digested with *Pac*I and transfected into 293 cells plated in a 60-mm dish with SuperFect (Qiagen, Valencia, CA), according to the manufacturer's instructions. Viruses (Ad-H1-p53, Ad-H1-Myc, Ad-H1tetO-p53, and Ad-H1tetO-Myc) were prepared as described previously (Mizuguchi and Kay, 1998). Ad vectors containing only the H1 promoter sequence (without a target sequence) (Ad-H1 and Ad-H1tetO) were similarly prepared. Ad-TR, the Ad vector expressing TetR, had been previously prepared (Xu *et al.*, 2003a). Ad-null contains no transgene in the E1 deletion region. Virus was purified by CsCl₂ gradient centrifugation, dialyzed with a solution containing 10 mM Tris (pH 7.5), 1 mM MgCl₂, and 10% glycerol, and stored in aliquots at −70°C. Determination of virus particle titer and infectious titer (plaque-forming units; PFU) was accomplished spectrophotometrically by the method of Maizel *et al.* (1968) and by the method of Kanegae *et al.* (1994), respectively. The PFU-to-particle ratio was 1:56 for Ad-H1-p53, 1:58 for Ad-H1-Myc, 1:56 for Ad-H1tetO-p53, 1:65 for Ad-H1tetO-Myc, 1:36 for Ad-H1, 1:50 for Ad-H1tetO, 1:24 for Ad-TR, and 1:57 for Ad-null.

Adenovirus-mediated gene transduction

A549 and HepG2 cells (2 × 10⁵ cells) were seeded into a 12-well dish. The next day, they were transduced with the Ad vectors for 1.5 hr. The cells were cultured with medium containing various concentrations of Dox (BD Biosciences Clontech), a derivative of tetracycline. Tet system-approved FCS (BD Biosciences Clontech), a tetracycline-free serum that has been determined to be optimal for the tetracycline-controllable expression system, was used as the FCS.

Western blotting for p53 and c-Myc proteins

Cell extracts were prepared in lysis buffer (25 mM Tris [pH 7.5], 1% Triton X-100, 0.5% sodium deoxycholate, 5 mM EDTA, 150 mM NaCl) containing a cocktail of protease inhibitors (Sigma, St. Louis, MO). The protein content was measured with an assay kit from Bio-Rad (Hercules, CA), using bovine serum albumin as the standard. Protein samples (10 μg) were electrophoresed on 12.5% sodium dodecyl sulfate (SDS)–polyacrylamide gels under reducing conditions, followed by electrotransfer to Immobilon-P membranes (Millipore, Bedford, MA). After blocking in Block Ace (Dainippon Pharmaceuticals, Osaka, Japan), the filters were incubated with antibodies against p53 (Santa Cruz Biotechnology, Santa Cruz, CA), c-Myc (Santa Cruz Biotechnology), and actin (Oncogene Research Products, San Diego, CA), followed by incubation in the presence of peroxidase-labeled goat anti-mouse IgG antibody (American Qualex Antibodies, San Clemente, CA) or peroxidase-labeled goat anti-mouse IgM antibody (Oncogene Research Products). The filters were developed using chemiluminescence (ECL Western blotting detection system; Amersham Biosciences, Piscataway, NJ). Signals were read with an LAS-3000 (Fujifilm, Tokyo, Japan), and quantified by Image Gauge software (Fujifilm).

Northern blot for p53 and c-myc siRNAs

Total RNA was isolated with ISOGEN reagent (Nippon Gene, Tokyo, Japan) according to the manufacturer's instruc-